KeAi
CHINESE ROOTS
GLOBAL IMPACT

Contents lists available at ScienceDirect

Petroleum Science

journal homepage: www.keaipublishing.com/en/journals/petroleum-science



Original Paper

Rock breakage and temperature rising of rock cutting after hightemperature treatment



Can Cai ^{a, b, c, d, *}, Wen-Yang Cao ^b, Xian-Peng Yang ^{a, b, d}, Quan-Gong Xie ^b, Bang-Run Li ^b, Zheng-Bo Tan ^b, Chun-Liang Zhang ^b, Chi Peng ^{a, b}, Hao Chen ^{a, b, d}, Yu-Long Zhao ^{a, b}

- ^a The State Key Laboratory of Oil&Gas Reservoir Geology and Exploitation, Southwest Petroleum University, Chengdu, 610500, Sichuan, China
- b Laboratory of High-pressure Jet Theory and Application Technology, School of Mechanical Engineering, Southwest Petroleum University, Chengdu, 610500, Sichuan. China
- ^c School of Engineering, University of Aberdeen, Aberdeen, AB24 3FX, United Kingdom
- ^d Geothermal energy research center, Southwest Petroleum University, Chengdu, 610500, Sichuan, China

ARTICLE INFO

Article history: Received 17 April 2024 Received in revised form 11 February 2025 Accepted 13 February 2025 Available online 14 February 2025

Edited by Jia-Jia Fei

Reywords:
High-temperature treatment
Hot dry rock well drilling
Rock breakage
Temperature variation
Heat generation

ABSTRACT

Geothermal energy is a clean and ecologically friendly energy source with significant potential. The temperature variations between the Polycrystalline Diamond Compact (PDC) cutter and the rock of the reservoir are the key factors affecting the cutting performance when drilling through formations with thermally damaged rock. To better investigate the temperature rise, a series of rock samples treated at high temperatures (9-300 °C) were broken with a PDC cutter. The performance of the PDC cutter on these samples was studied using cutting force sensors, high-speed photography, and the thermal infrared imager. Based on the experimental data, a new cutting force evaluation parameter, η , is suggested. The link between the cutting force and rock properties is discussed in detail. The present results indicate that the average cutting force of high-temperature-treated granite is 3-5 times that of the thermally damaged sandstone. Furthermore, a critical temperature for thermal damage has been identified in granite cutting at 100–200 °C and in sandstone at 100 °C. This corresponds to the temperature at which interlayer water loss and thermal crack closure occur. The results also indicate that when the treatment temperature exceeds the critical threshold, both the cutting force and temperature rise exhibit more significant changes with increasing temperature. Additionally, the maximum temperature of the PDC cutter during granite cutting can reach 47.6 °C, which is almost 34 °C higher than that of sandstone. Regarding debris size, granite is much less sensitive to the treatment temperature, showing only slight changes in debris size compared to sandstone as the treatment temperature increases. The increasing cutter-rock interface area can significantly reduce frictional heat generation while increasing the cutting force and enhancing the temperature rise. The parameter valuation of the newly defined parameter η , which is related to frictional heating, shows that the capacity of the thermal generation and the heat transfer change as the temperature rises at the cutter-rock interface. At last, the correlation analysis indicates that the cutting force of sandstone and granite is highly correlated with σ_r^2/σ_c , E/σ_c and σ_r . This study serves as a theoretical support and technical guidance for cutting hot dry rock (HDR), which is of great significance to HDR drilling.

© 2025 The Authors. Publishing services by Elsevier B.V. on behalf of KeAi Communications Co. Ltd. This is an open access article under the CC BY-NC-ND license (http://creativecommons.org/licenses/by-nc-nd/4.0/).

1. Introduction

Effectively cutting thermally damaged rock has a wide range of applications in deep well drilling, especially in HDR well drilling, where PDC drill bits are the preferred drilling tools (Pessier and

* Corresponding author. E-mail address: cainia10@163.com (C. Cai). Damschen, 2011). In particular, a large number of deep wells have been drilled recently, showing that the requirement for high efficiency in cutting thermally damaged rock is a significant challenge due to the rapid failure of drill bits within a short operational period (Agostini, 2020; Cirimello et al., 2018). Besides, HDR wells also require an efficient and long-lasting bit capable of preventing thermal wear (Zhao et al., 2015; Liu, 2017). Therefore, many studies have been conducted in the past to address this issue.

A meticulous literature review indicates that the first strategy to

extend the life cycle of the drill bit is to optimize the design of the drill bit based on thermally damaged rock drilling (Galarraga, 2016). Cai et al. (2023) investigated the cutting process of PDC cutters with varying degrees of wear and found that the cutting temperature significantly increases after the PDC cutters become worn. Those studies indicate that the substantial wear of the cutter is one of the main reasons that cause the failure of the PDC bit in the above well drilling scenarios, especially the thermal wear (Apple et al., 1993; Tze-Pin et al., 1992). When the rock with a high temperature in the well bottom is cut by the PDC cutter, the thermal wear experienced by the cutter is a serious problem that leads to the reduction of cutting efficiency that needs to be studied carefully. Thus, it is urgent to investigate the cutting mechanism of the PDC cutter, including the cutting debris stripping, the cutting force response and the temperature change.

To deal with the above concerns, early research in this field was focused on the single PDC cutter cutting. The single cutter experiment was primarily conducted in the 1970s (Cheatham and Daniels et al., 1979) and later developed into a practical method to investigate the rock breakage mechanism, in order to optimize the operating parameters and drill bit design (Zijsling et al., 1987). The establishment of a mechanical single-cutter cutting model is fundamental to study the single cutter experiment. Thus, Li et al. (2020) proposed the PDC cutting gear mechanics model by modifying the Nishimatsu model, taking the in-situ stress into consideration. In their study, a new model that combined the mechanical properties of the rock and the rock crushing was used to simulate the cutting process and evaluate the capacity of the drill bit. Wang et al. (2019) studied the stress response of the PDC bit in the drilling process and investigated the microscopic characteristics and temperature variation of the interacting surface between the rock and the PDC cutter. They also proposed a numerical model to calculate the actual contact area between the PDC bit and the formation. Cheng et al. (2018) proposed a new theoretical model to analyze the cutting force and the failure mechanism of the rock based on the stress theory. The cutting force predicted by this model was verified by the experimental results. According to their research, there is a curly surface of the rock that results in elongated debris.

The cutting process of the PDC cutter is not only influenced by the cutting force but also the temperature variation. It is believed that the formation temperature and the heat generation in the cutting process play an important role in rock crushing. Early research in this field focused on using the hybrid boundary value heat transfer problem to analyze the heat transfer of the PDC cutter during two-dimensional orthogonal rock cutting under steadystate conditions (Che et al., 2015). A mathematical model regarding the temperature field of the intermittent cutting of the PDC cutter was established by Deng et al. (2011) to investigate the temperature variation of the PDC cutter in the rock cutting process by experimental studies. In their study, the temperature distribution of both the alumina ceramic specimen and the PDC cutter working surface was simulated by the finite element method and verified by experimental results. Zhu and Dan (2019) investigated rock breakage during the PDC cutting process using numerical simulations that considered high temperature and confining pressure. Their results showed that the rock-breaking efficiency of the PDC cutter decreased with increasing cutting depth. Additionally, it increased initially but then decreased with rising temperature, with the critical temperature of high-pressure rock being 200 °C.

The influences of drilling parameters on the rock-breaking energy consumption of the PDC cutters were investigated by Zhao et al. (2009) under high temperature and pressure by using experiments. Their research clearly showed how rock-breaking efficiency and energy efficiency change under high temperatures and pressures. Meanwhile, early numerical studies used the finite

element method to calculate the heat transfer between the rock and the PDC bit (Prakash et al., 1989), in which the single-cutter experimental results were used to verify simulation results. The effects of the film coefficient, the diamond thickness and other technological parameters on the internal temperature distribution of the PDC cutter were also studied. To illustrate the temperature variation of the drill bit and different factors influencing rock cutting performance, Yang et al. (2011) were the first to develop a numerical model with differential equations based on the analysis of heat transfer during the drilling process. In addition, Liu and Zhu (2019) studied the stress response and cutting debris formation during the PDC cutting process through experiments under different cutting depths, cutting speeds and rake angles, and obtained how cutting parameters affect the formation of the cutting debris.

With the advancement of technology, many scholars have begun using advanced equipment to conduct their research. For example, detailed observation of the PDC cutter cutting was successfully obtained by Che et al. (2017) and Cheng et al. (2018) by using high-speed photography, which helps better evaluate the rock-breaking efficiency. In conclusion, according to all the studies reviewed in this paper, the main types of rock failure during the PDC cutter cutting process are brittle failure and tensile failure. Furthermore, it is possible for both types of failure to coexist within the same cutting process, which mostly depends on the rock property being cut and the cutting condition. And at last, the friction between the PDC cutter and the rock is the primary cause of the temperature rise that occurs throughout the cutting process, especially when cutting the brittle rock.

The extensive studies in the past about the PDC cutter cutting process and its mechanism have helped scholars in this field conclude that the temperature rise during the PDC cutting process is the determining factor for rock breaking efficiency. While the importance of the temperature rise during the PDC cutting has been widely recognized, the law of this temperature rise in the heat-treated rock cutting remains unclear. Besides, the industrial requirements of HDR well drilling make it urgent to investigate the rock breakage and the temperature variation in HDR cutting. Therefore, a series of experiments were designed in the present study using various experimental tools, including strain gauges, high-speed photography, and thermal infrared imaging techniques. Additionally, to observe the cracks and temperature variations in the cross-section of the formation, where the PDC cutter axis is located, half-cutting experiments were conducted. The effects of different temperatures, rock sample properties, and cutting methods on the cutting force, the cutting temperature rise, and the rock debris size and shape were analyzed. The heat generation and the relationship between the rock properties and the cutting force were also thoroughly investigated.

Scholars have researched the PDC cutter cutting tests and mechanical model extensively. In this process, it was gradually realized that the temperature rise during PDC cutting is a significant factor affecting the rock-breaking efficiency. While the temperature rise during PDC cutting has been recognized, the law of this temperature rise in heat-treated rock cutting remains unclear. The industrial requirements of HDR well drilling make us realize that it is urgent to explore the problem of rock breakage and temperature variation in HDR cutting. Therefore, a series of experiments are designed considering various measurement methods, including strain gauges, high-speed photography, and thermal infrared imaging. Additionally, to observe the cracks and temperature variations in the cross-section where the PDC cutter axis is located, semi-cutting experiments are conducted. The effects of different temperatures, rock samples, and cutting methods on cutting force, cutting temperature rise, and rock debris size are analyzed. We

thoroughly discuss heat generation and the relationship between rock properties and cutting force. A new evaluation parameter η , related to frictional heat generation has been proposed to better reflect the thermal response during the rock cutting process. Additionally, a self-developed Python program was used to analyze the relationship between rock characteristics after thermal damage and cutting forces.

2. Rock samples and experimental program

2.1. Experimental setup

The total torque of the PDC bit is known to consist of the contributions from all cutters. Therefore, the cutting mechanism of the PDC bit can be exposed by estimating the cutting performance of each cutter (Akbari, 2011; Yahiaoui et al., 2016a, 2016b; Warren and Sinor, 1994; Akbari and Miska, 2016). The experimental setup shown in Fig. 1 was designed using various measuring methodologies in this study to simulate the rock cutting of the PDC cutter. In this experimental facility, the experiment can be carried out at various cutting parameters, such as the cutting depth, cutting speed, rake angle, side angle and cutter diameter, and three primary testing methods were employed in the present rock cutting scenarios. The linear cutting experiments were monitored using axial, tangential, and radial strain gauges, respectively, which have been successfully practiced before (Shi, 2006; Huang et al., 2019). In addition, direct observations of the short-term cutting process were allowed by high-speed photography with a maximum image rate of 200,000 frames per second, which is sufficient to help reveal the generation and removal of cutting debris in the rock. The temperature variation during rock cutting was monitored using a thermal infrared imager. Besides, the cutting temperature in the experimental field is determined based on the ambient temperature and the temperature captured by the thermal infrared camera. Besides, the temperature variation of PDC cutter during the rock cutting was monitored using a thermal infrared imager. Finally, the size and shape of the debris during the cutting process were characterized using a reference object (coin).

Before experiments, rock specimens were thermally treated for at least 4 h in the temperature range of 100–300 °C, and then slowly cooled in the air environment at room temperature, the rock temperature gradually cooled to room temperature (9 °C). To meet the designited experimental condition, the rock specimens were fixed in the block with the designed cutting depth, rake and side angle, with all the monitoring sensors and facilities, including the strain gauges, the high-speed photography, and the thermal infrared imagers carefully prepared. As mentioned earlier, multiple strain gauges were used to detect the axial, tangential and lateral forces of the PDC cutter in this experiment, and the cutting velocities of all test groups were set constant at 460 mm/s.

Fig. 2 is the schematic diagram of cutting with the PDC cutter, which illustrates the rock-breaking mechanical model and the heat generation locations of the PDC cutter. For the PDC cutter, the main forces are active in the axial direction and tangential direction, respectively, and are measured by the sensors.

According to Shi's research (Shi, 2006), three groups of strain gauges were used to monitor the cutting force, and the relationship between the monitoring force and digital data can be obtained (Akbari, 2014; Detournay and Defourny, 1992; Dougherty et al., 2015; Glowka, 1989). Such an approach has been successfully applied before (Huang et al., 2016, 2019), and the three directional forces can be calculated using the following equations of strain:

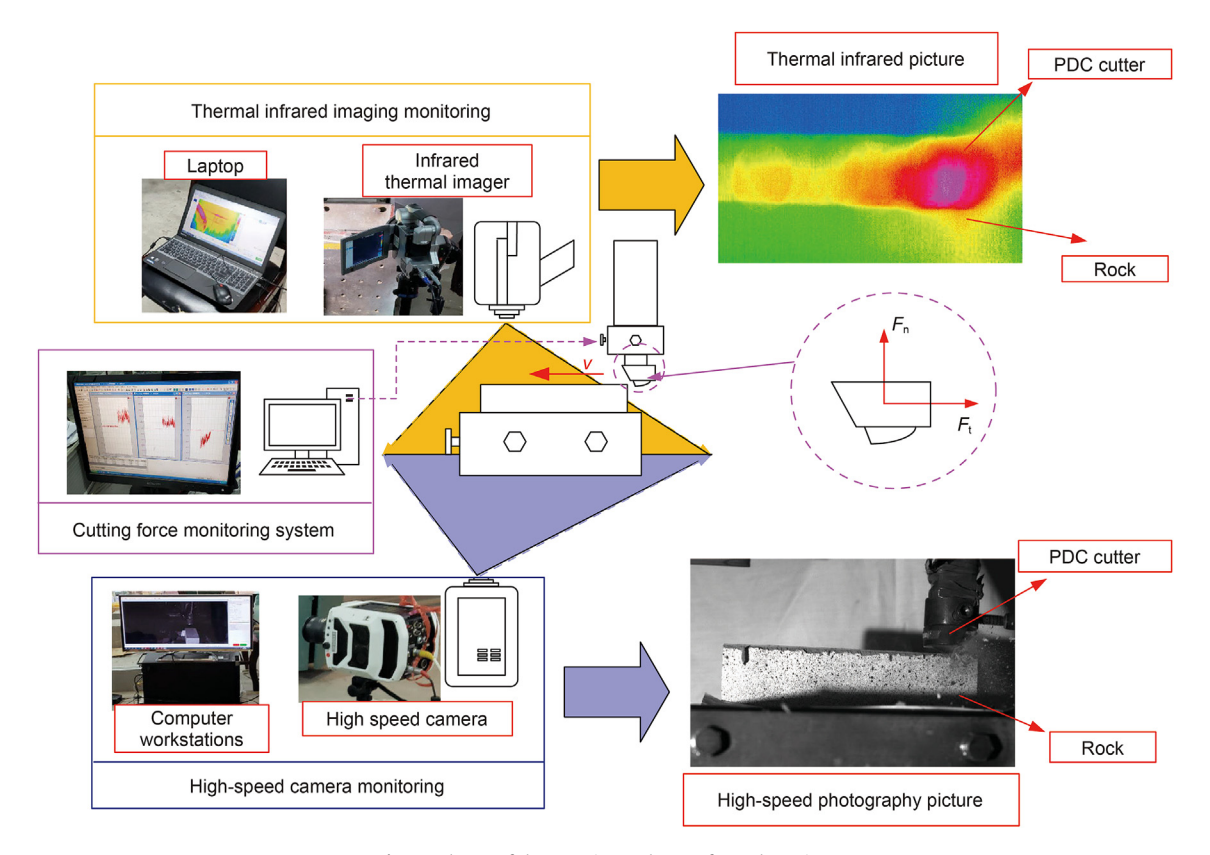


Fig. 1. Scheme of the experimental setup for rock cutting.

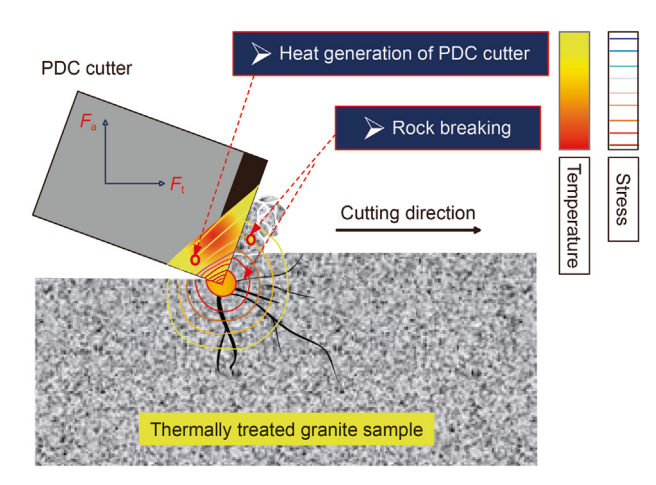


Fig. 2. The two-dimensional cutting model of PDC cutter.

$$\begin{cases} F_{\rm N} = 16.309u_{\rm a} + 0.4224031u_{\rm t} - 0.1321029u_{\rm r} \\ F_{\rm t} = 2.4383848u_{\rm a} + 0.8764u_{\rm t} + 11605942u_{\rm r} \\ F_{\rm r} = 0.34264986u_{\rm a} + 0.012392u_{\rm t} + 2.0654u_{\rm r} \end{cases} \tag{1}$$

where F_N , F_t and F_r are axial, tangential and lateral forces, respectively. In our experiments, the tangential force applied to the cutting direction is also named the cutting force; u_a , u_t and u_r are the electrical signals in the axial, tangential and radial direction.

In the previous study, the linear cutting was carried out in the thick rock samples (Rostamsowlat et al., 2019), where only the rock breakage at the top surface of the rock sample is investigated (Rostamsowlat et al., 2019; Yahiaoui et al., 2016; Richard et al., 2010). Whereas, in our experimental, the rock samples were divided into two groups, including the thin plate and thick plate cutting, to simulate the rock breakage of both the top surface and center section (see the blue section in Fig. 3(a) and red section in Fig. 3(b)). To make it easy to observe the rock breakage and temperature variation in the center section, the cutting groove of the thin plate specimen is only half of that of the thick plate specimen, as shown in Fig. 3(b). The thin plate sample is cut by the PDC cutter,

allowing high-speed photography to observe the initiation and propagation of cracks in the section along the cutting direction. Additionally, it is convenient for observing the temperature variation of both the PDC cutter and the rock specimen. The thick plate sample is used to study the crack generation on the top surface, as shown in Fig. 3(a).

2.2. Rock sample treatment

Attributing to their extensive distribution and adaptability. sandstone and granite are widely used in geothermal engineering. such as HDR well drilling. Sandstone is a sedimentary rock that is formed by the cementation and compaction of weathered sediments, whereas granite is an igneous rock formed by liquid magma entering the upper crust and slowly condenses and crystallizes. The different ways of formation lead to their extremely different diagenesis and interior structures. As a result, temperature affects the tensile strength of each rock quite differently. To this end, both types of rock were prepared as experimental materials in this study to better understand their mechanical behaviors during the PDC cutting process. Additionally, two different shapes of rock specimens were manufactured. The first shape is a thin plate rock with dimensions of 280 mm in length, 16 mm in width, and 202 mm in height, making it convenient to observe the process of crack initiation and block removal from the left side when the PDC cutter starts breaking the plate. The second shape is a rectangular solid sample with a size of 280 mm \times 150 mm \times 202 mm (length, width, height). All manufacturing surface error of specimen is within ±0.1 mm. Then, to clearly capture the process of rock breaking by high-speed photography, the monitoring side of the sample is covered by the spray paint. Fig. 4 displays the painted surface before-and-after treatment. These thin plate rock samples and rectangular rock samples were cured at high temperatures of 100. 200, and 300 °C, respectively, for over 4 h at a constant heating rate. They were held at the target temperature for at least 4 h and then allowed to air cool to room temperature. This method of thermal treatment has been widely used before by scholars (Sun et al., 2016; Sha et al., 2020; Zhang et al., 2021). In the experimental diagram, the comparative group is the sample without heated damage in environmental temperature (9 °C).

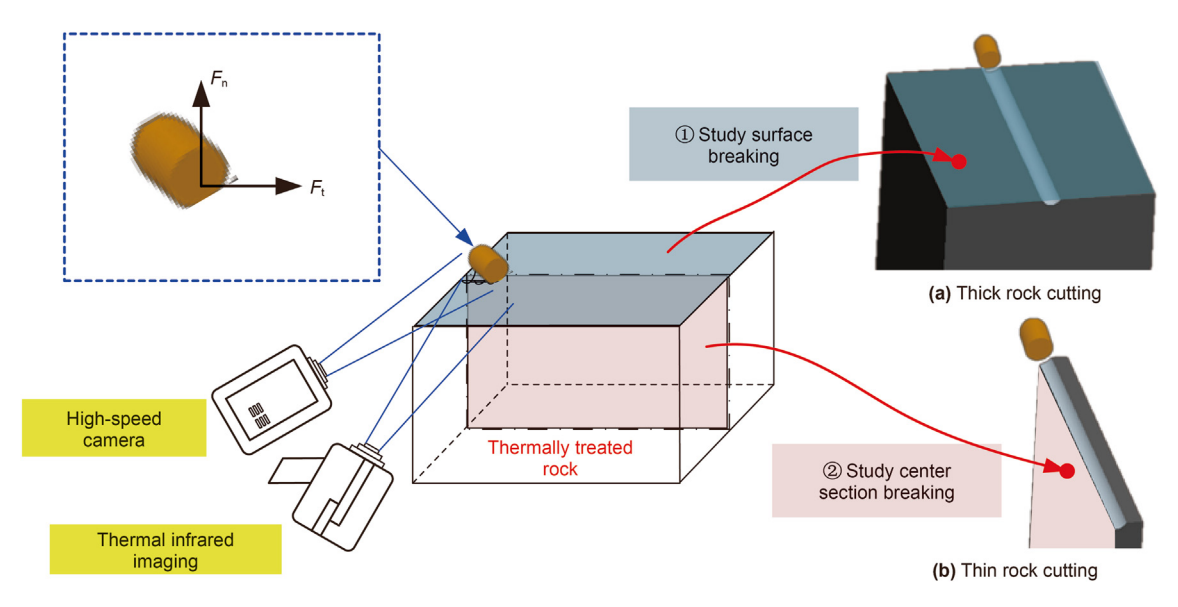


Fig. 3. High-temperature rock (100, 200, 300 °C etc.) cutting by using PDC cutter. (a) Thick rock cutting to study the surface breaking, (b) Thin rock cutting to study the center section breaking.

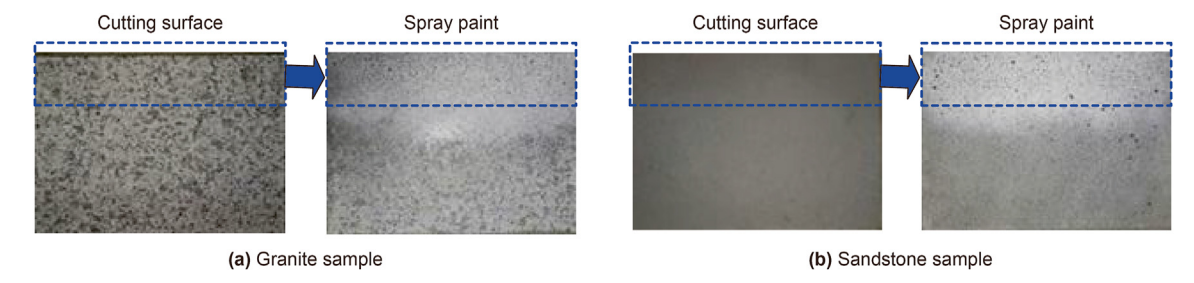


Fig. 4. Preparation and pre-treatment on the cutting surface of rock specimen.

To measure the rock mechanical properties, cylindrical rock specimens (50 mm in diameter and 100 mm in length) and Brazilian splitting test samples (50 mm in diameter and 25 mm in height) were drilled from the granite and sandstone samples. Then, the rock samples after high temperature treatment were tested to obtain the uniaxial compressive strength (UCS), Young's modulus (E) and tensile strength (TS), using the Rock and Concrete Mechanical Test System (Model: *RMT301*) by the American Society for Testing and Materials (ASTM) standards. The above average rock properties are calculated according to 2 data sets at the same treatment temperature, and are shown in Table 1.

2.3. Experimental program

The experimental program is shown in Table 2. Three experimental groups were designed to investigate the effects of rock type, heating the temperature and cutting width on the rock breakage and temperature variation, respectively. First, the rock samples of each group were set in the high-temperature heating furnace (see Fig. 5) and heated to 100, 200 and 300 °C. The heating rate was 10 °C/min and after reaching the target temperature, a constant temperature is maintained for 4 h to ensure adequate heating. Secondly, the control group of the rock sample was kept at an environmental temperature (9 °C) without heating. After hightemperature treatment, all rock samples were cooled in room temperature for over 24 h. At last, if the usual cutting method is used, the breakage and temperature variation on the section where the axis of the PDC cutter is located cannot be observed. Two different cutting schematic programs were designed for our experiments: half-cutter cutting and whole-cutter cutting (see Fig. 6). Besides, other cutting parameters and cutter structure remain constant. The thin rock specimen was cut by a PDC cutter to a depth

of 3 mm and a width of half the cutter diameter. The cutting depth of the thick rock sample was 2 mm with a full cutter width, as shown in Table 2. All cutters in the experiments have the same diameter. The back rake angle of the cutter was set constant at 9° . During the cutting, the cutting force (the tangential force of F_t in Fig. 3) was recorded by strain gauges. And the output signal was processed using the Fast Fourier Transform (FFT) filter with a cut-off frequency of 0-45 Hz.

3. Results

3.1. Temperature effects on rock mechanical properties

Many studies find that the rock mechanical properties gradually change with increasing temperature (Xu et al., 2014; Oin et al., 2020; Hu et al., 2018). According to the experimental results, the UCS of the sandstone decreases up to 100 °C and then increases with further temperature rise beyond 100 °C (Fig. 7(a)). This is due to the evaporation of interlayer water within the rock during the heating process from 0 to 100 °C, which leads to an increase in internal fractures, thereby resulting in the deterioration of the mechanical properties. Meanwhile, the TS of the sandstone increases as temperatures rise below 300 °C (Fig. 7(b)), while the E decreases linearly with temperature below 200 °C and remains unchanged above 300 °C (Fig. 7(c)). However, the mechanical properties of granite show different varied trends. It is found that in the range of room temperature to 300 °C, TS reduces as temperatures increase (Fig. 7(b)). UCS and E increase up to 100 °C and then decrease with further temperature rise (Fig. 5(a) and (c)). Both the interlayer water and mineral expansion affect the variation of rock mechanical properties. At relatively low thermal temperature damage, the tensile strength of sandstone would be weakened if

 Table 1

 The average value of rock properties. (The rock property of the comparative group without heated damage is also measured, which is marked in gray color in the table.)

Rock types	Treated temperature, °C	Density before heating, g/cm ³	Young's modulus, GPa	Tensile strength, MPa	Uniaxial compressive strength, MPa	Mass loss after heating,
		=	_			-
Granite	Room temperature (9)	2.605	6.17	4.56	80.13	1
		2.625	5.83	4.97	74.34	1
	100	2.617	9.84	3.80	81.73	0
		2.646	8.82	4.93	98.92	0
	200	2.634	5.29	4.01	56.56	1.87
		2.618	5.21	4.04	52.80	1.89
	300	2.633	5.48	4.11	57.43	1.87
		2.626	4.87	3.90	57.20	3.00
Sandstone	Room temperature (9)	2.264	3.52	1.94	22.99	1
		2.263	2.21	1.61	23.13	1
	100	2.278	2.26	1.67	21.39	6.48
		2.274	2.47	1.98	20.00	6.47
	200	2.254	2.05	2.34	27.30	12.99
		2.214	1.91	2.13	23.13	13.19
	300	2.272	2.29	2.67	24.27	10.82
		2.280	2.28	2.97	29.61	13.01

Table 2 Experimental program of PDC cutting (*Bold means the varied parameters*).

Group item	Rock sample	Cutting width	Cutting depth, mm	Cutter diameter, mm	Treated temperature, °C
1	Sandstone	Half-cutter	3	19	Environmental temperature (9 °C) 100 200 300
2	Granite	Half-cutter	3	19	Environmental temperature (9 °C) 100 200 300
3	Sandstone	Whole-cutter	2	19	Environmental temperature (9 °C) 100 200 300



Fig. 5. High-temperature heating furnace.

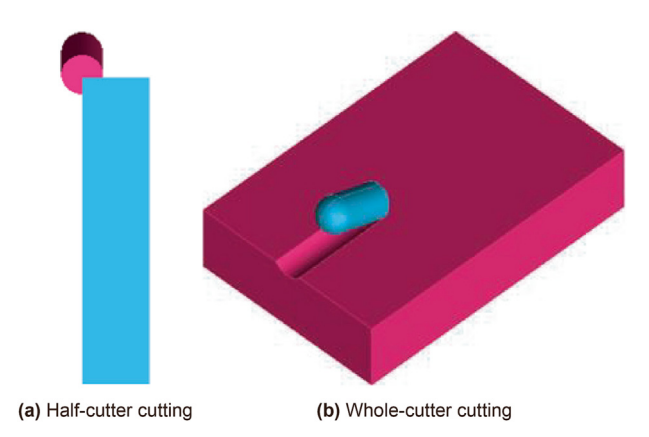


Fig. 6. Schematic diagram of cutting program.

the influence of interlayer water is more significant than the mineral expansion (Sha et al., 2020). However, since granite has fewer original microcracks than sandstone, the minerals have limited space to expand when temperatures rise (Sha et al., 2020). Therefore, the microcracks in granite are completely closed at 100 °C. As

the temperature continues to rise, the thermal stress caused by mineral expansion becomes the major influencing factor, resulting in a decrease in the strength of the granite. Nevertheless, it is noted that there is a small rise in Young's modulus and UCS before $100\,^{\circ}$ C, as also observed by Yang et al. (2017a, 2017b), Huang et al. (2017) and Qin et al. (2020). This is because the main crack closure is caused by mineral expansion at the critical temperature, which is typically around $100\,^{\circ}$ C.

3.2. Temperature effect on cutting force

As it has been widely recognized that the mechanical strength of rock after heating is reduced due to micro and macro damage (Gautam et al., 2016; Yang et al., 2017, 2019; Chen et al., 2017). It is necessary to evaluate the cutting force of PDC when cutting the high temperature treated specimens.

(1) Granite cutting

The cutting force of the PDC cutter, including the axial and tangential forces, was measured by sensors during the cutting of high-temperature treated samples. To eliminate the influence of data noise caused by surrounding factors, the output signals were processed and smoothed by using the Fast Fourier Transform (FFT) filter with a cut off frequency of 0-45 Hz. According to the results of the axial and tangential forces in Fig. 8, the cutting force rapidly increases to its maximum in a short time when the rock being cut is not heat treated. However, the cutting force of the heat treated rock increases slowly compared to rock at room temperature. Surprisingly, the maximum axial and tangential forces are 7335 and 7980 N, respectively, which are 5.3 and 6.7 times those of the heated rock, According to Zhou et al. (2017), the rock properties are strongly related to the cutting force (also known as horizontal force). Earlier in Section 3.1, the rock properties are affected by interlayer water loss and thermal crack initiation after high temperature treatment, resulting in an apparent deterioration of rock properties and substantial reduction of maximum cutting force. That is why the force is greater at the treated temperature of 9 °C than at the 100-300 °C. Thus, heating the rock is beneficial, as it reduces the cutting force, finally improving the drilling efficiency. The variation curves also indicate that the cutting force of rock at room temperature is higher than that of heated rock when the cutting time varies from 0.02 to 0.1 s. This is due to the reduced strength of the heated rock, which results in easier and softer penetration during the first 0.15 s of cutting. The effect of the property reduction on cutting force will be deeply discussed in Section 4.

Due to the movement of cutting debris and the vibration of cutter, the cutting force fluctuates with time. Therefore, the average

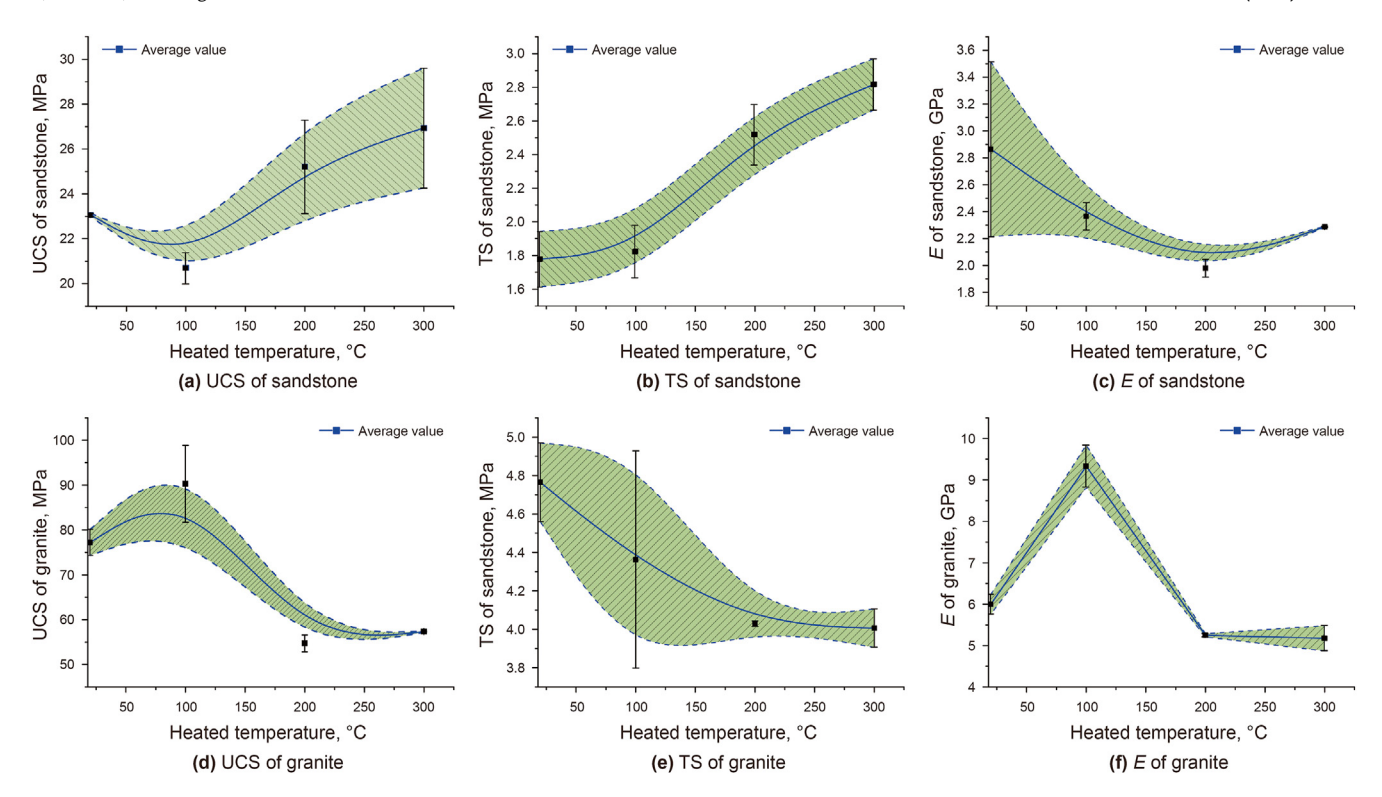


Fig. 7. The variation of mechanical properties with increasing treatment temperature.

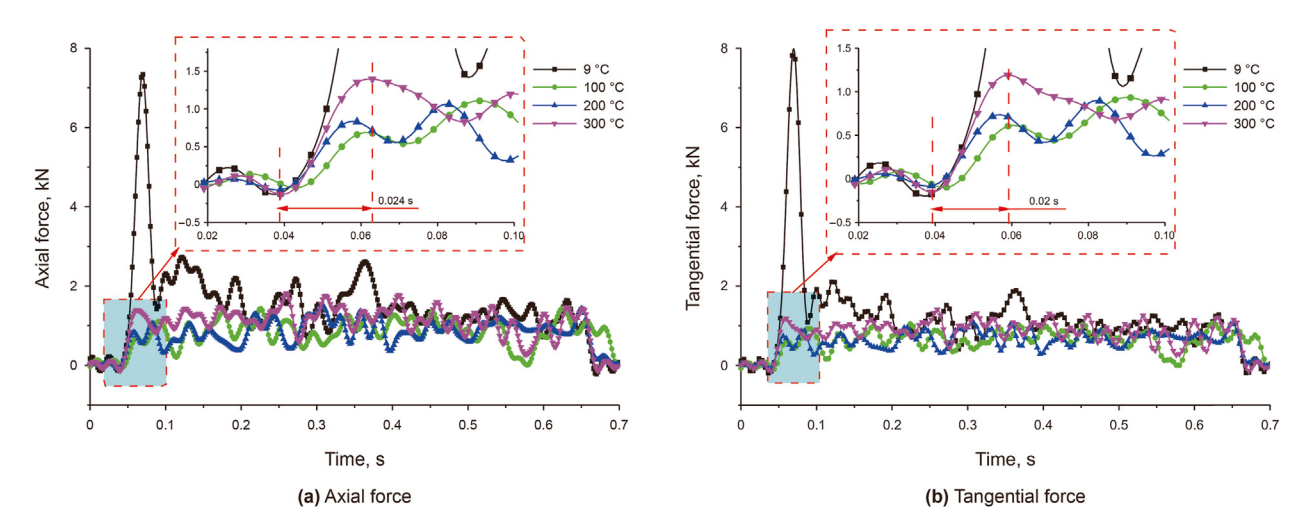


Fig. 8. The variation of cutting force during cutting granite with different treatment temperatures.

cutting force in cutting terms is commonly used to evaluate the cutting performance (Liu and Zhu, 2019; Shi, 2006). Thus, the average values of both axial and tangential forces were calculated according to Fig. 8, and displayed in Fig. 9. It can be seen that there is a similar varying trend for both the axial and tangential forces of the PDC cutter, which quickly drops with increasing treated temperature and then smoothly grows when the treatment temperature exceeds 100 °C. The results also show that the average axial and tangential force at 100 °C are 54.6% and 52.1% of the maximum average value, respectively, at room temperature. With the increasing treatment temperature, the average axial and tangential force at 200 °C is approximately the same as the value at 100 °C. However, it is found that the average cutting force can increase

when the treatment temperature of granite rises to 300 $^{\circ}$ C, which is 69.6% and 67.6% of the maximum average cutting force, respectively. Therefore, it is rational to conclude that there is a critical treatment temperature for the granite, assuredly between 9 and 200 $^{\circ}$ C, which leads to a sharp reduction in the cutting force for the PDC cutter. We can see that this conversion temperature falls within the range of the critical temperature for rock property variations, as shown in Table 1 and Fig. 5.

Several factors are known to affect the rock properties and cutting force. Most scholars have found that as treatment temperature increases, both Young's modulus and strength drop. Chen et al. (2017) and Yang (2017) have concluded that the mechanical properties of granite apparently degraded when it was heated to

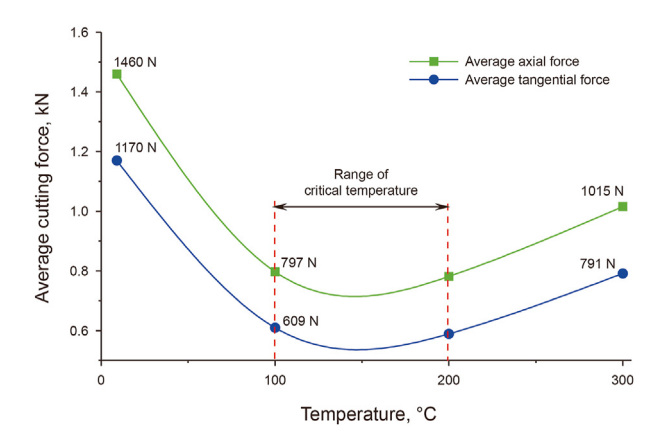


Fig. 9. The variation of average cutting force with increasing treatment temperature.

over 200 °C. However, some studies also found that the strength would increase at temperatures of 150 °C (Huang et al., 2017), 100 °C (Sha et al., 2020) or 75 °C (Xu and Liu, 2000) due to the crack close or interlayer water loss, and the porosity of the granite specimens increased at 100 °C because of the interlayer water loss (Qin et al., 2020; Sha et al., 2020). The mass loss of granite specimens after high-temperature heating also supports the above conclusions (See Table 1). Thus, both thermal crack closure and interlayer water loss are believed to be the main factors determining the variation in cutting force and the critical temperature. The thermal crack close at temperatures from 75 to 150 °C contributes significantly to the decrease of average cutting force. The water loss also has an important impact on the lowest cutting force at 150 °C.

(2) Sandstone cutting

Similarly, the cutting force of the PDC cutter while cutting sandstone was also tested and recorded. As can be seen from Fig. 10, the axial and tangential forces of the sandstone at the treatment temperature of 100 °C are obviously larger than those at room temperature, 200 and 300 °C. Interestingly, the PDC cutter has a lower cutting force than that of other groups when cutting the sandstone at a treatment temperature of 300 °C. On the other hand,

the comparison between the four variation curves of both axial and tangential forces indicates that the group with a temperature of $100\,^{\circ}\text{C}$ exhibits more extreme fluctuations than the others. And the cutting force fluctuation of the heat treated sandstone is more apparent than that of untreated sandstone. Therefore, it is concluded that the heated sandstone tends to produce a significantly higher cutting force with more fluctuations than that of the untreated sandstone.

According to the cutting force variation, the average value of axial and tangential forces was calculated and displayed in Fig. 11. The variation of average axial force and average tangential force align with each other with increasing treatment temperature. It can be seen clearly that the average cutting force rises from 173 N to the peak value of 257 N when the treatment temperature increases from room temperature to 100 °C. When the temperature of the heated sandstone exceeds 100 °C, the average cutting force of the PDC cutter starts to reduce. Numerous laboratory experiments have shown that the rocks have an obvious brittle-ductile transition as treated temperature rises (Ding et al., 2016). In our research, the temperature at which of the brittle-ductile transition occurs is close to the temperature of the highest cutting force. Therefore, it is believed that there is a relatively lower critical treatment temperature close to 100 °C, where the cutting force is extremely higher than that in other cases. Similar to granite, the interlayer water and the thermal expansion of minerals caused by high temperatures together play an important role in the rock strength and cutting force. In Fig. 11, the results also show that at relatively low treatment temperature, the cutting force would increase due to the thermal expansion of minerals and water loss, which leads to an enhancement of compactness and strength. With the increase in treatment temperature, the influence of mineral dehydration becomes greater than that of mineral expansion (Sha et al., 2020), resulting in a gradual reduction of cutting force. For HDR well drilling, this observation indicates that heating the sandstone above 100 °C is more beneficial for rock breaking by PDC cutting due to the reduction in cutting force.

Comparing the rock-breaking process of the granite and sandstone, it can be seen that there is a great gap in the cutting force between granite and sandstone during PDC cutting. The granite specimen has a stronger mechanical strength than the sandstone specimen, making it more difficult to break with a PDC cutter under the same cutting conditions. The comparison of the average cutting

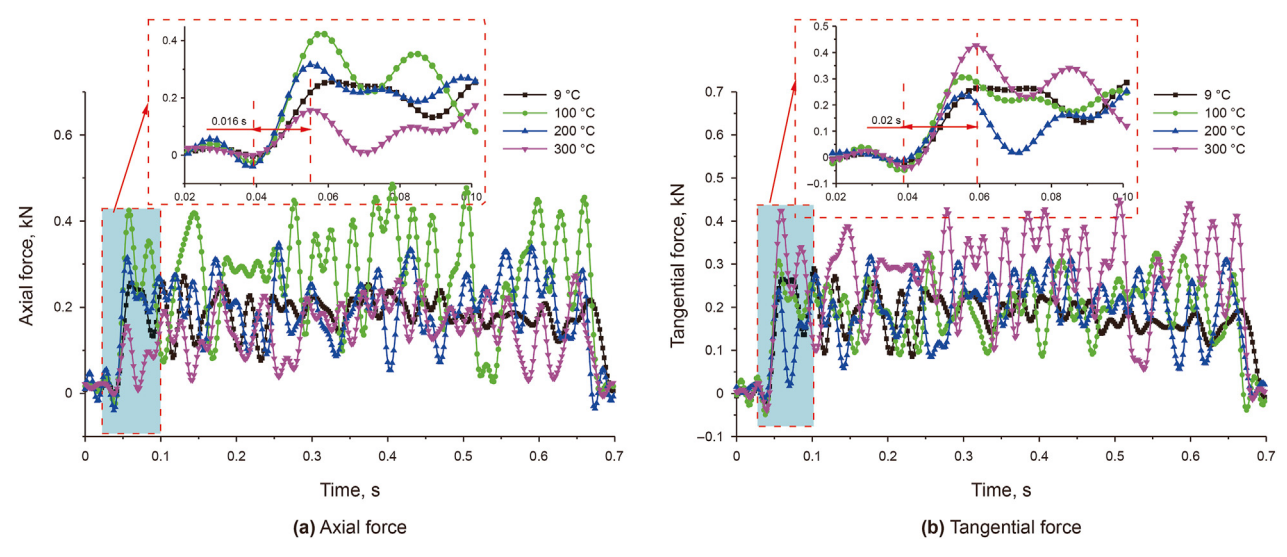


Fig. 10. The variation of cutting force during cutting sandstone with different treatment temperature.

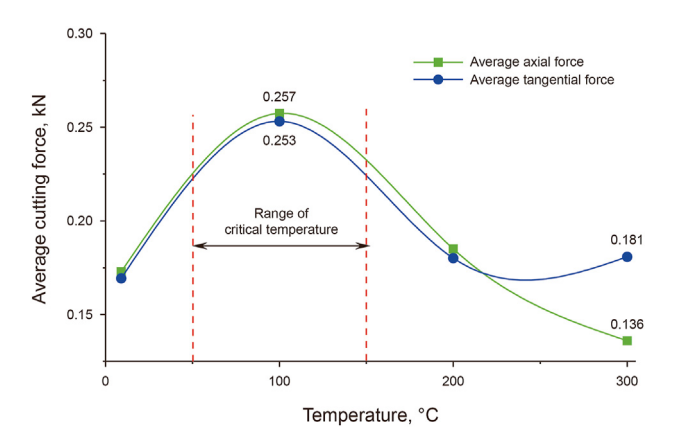


Fig. 11. The variation of average cutting force with increasing treatment temperature.

force between granite cutting (See Fig. 9) and sandstone cutting (Fig. 11) indicates that the average cutting force of granite ranges is 3—5 times higher than that of the sandstone sample. Moreover, the variation in the average cutting force of granite with increasing treatment temperature is also different from that of sandstone. The fact that two rock types show different trends in variations of the cutting force indicates that distinct influences of the treatment temperature on different rock types should be noticed. In addition, our results demonstrate that there is a critical temperature for both granite and sandstone, leading to a significant change in cutting force. The value of the critical temperature is strongly related to interlayer water loss and thermal crack initiation.

3.3. Temperature effect on PDC cutter heat generation

(1) Granite cutting

Some scholars have explored the temperature variation of the cutter while cutting rock. However, the effect of high temperature treatment on the temperature variation of the PDC cutter is still unknown. Each frame of the PDC cutter temperature is captured using a thermal infrared imager, and the temperature rise of the PDC cutter is collected as shown in Fig. 12(a). As can be seen from Fig. 12, the temperature rise of the PDC cutter first increases rapidly during the time from 0.033 to 0.166 s, and then gradually decreases. It is found that the temperature rise of the PDC cutter has the

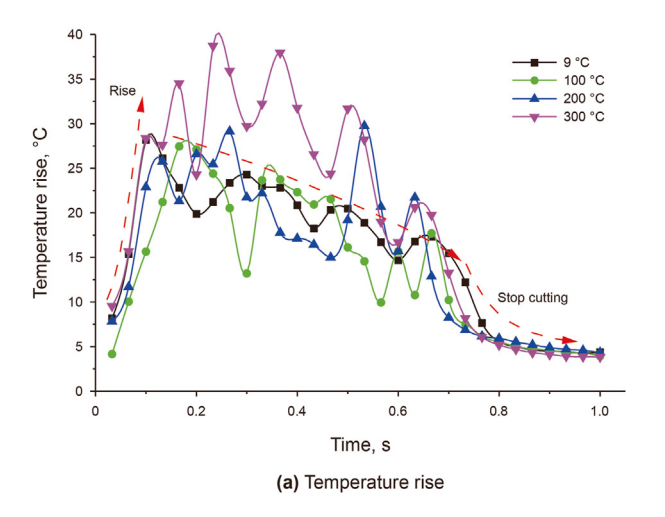
highest increasing rate when the granite is cut at room temperature and 300 °C treatment temperature. Under the influence of the heat generation and dissipation, the temperature rise of the PDC cutter fluctuates over the increasing cutting time. This fluctuation in temperature rise is caused by the periodic frictional heat and the removal of cutting debris. Comparing the four curves, It is found that the maximum temperature rise of the PDC cutter increases from 26.1 to 38.72 °C when the treatment temperature varies from 9 to 300 °C, suggesting a positive correlation between the temperature rise of the PDC cutter and increasing treatment temperature. Noticeably, the variation in temperature rise at the treatment temperature of 300 °C is different from other groups, indicating obvious effects of the high temperature of rock on the heat generation of the PDC cutter, which provides meaningful insights for high-temperature well drilling.

In addition, to further investigate the effect of treatment temperature on PDC cutter performance, the relative temperature difference between the high treatment temperature group and the untreated (room temperature) group was obtained. As shown in Fig. 12(b), the temperature difference is less than 0 °C when the cutter starts cutting during the time period between 0.033 and 0.166 s. At the starting stage of PDC cutter cutting, this temperature rise consists of cutting friction and rock deformation. When the cutter begins to penetrate the rock, there is a sharp deformation of the rock in a short time, resulting in significant heat generation. This makes rock deformation the major factor (compared to cutting friction) at the initial stage of PDC cutter cutting, determining the influence of treatment temperature on the cutter's temperature rise

Comparing the temperature difference of the three groups, it can be seen that when the heating temperature of granite is greater than 200 °C, the average value of temperature difference is remarkably larger than other groups. A conclusion can be drawn that there is a critical temperature between 200 and 300 °C that changes the cutting efficiency and cutting heat generation of granite significantly, which is in accordance with the results of granite cutting force before. It is generally believed that the mechanical properties of granite decline significantly after heating above 200 °C, and this critical temperature plays a crucial role in heat generation and the temperature rise of the PDC cutter.

(2) Sandstone cutting

Similarly, the temperature rise of sandstone cutting is also



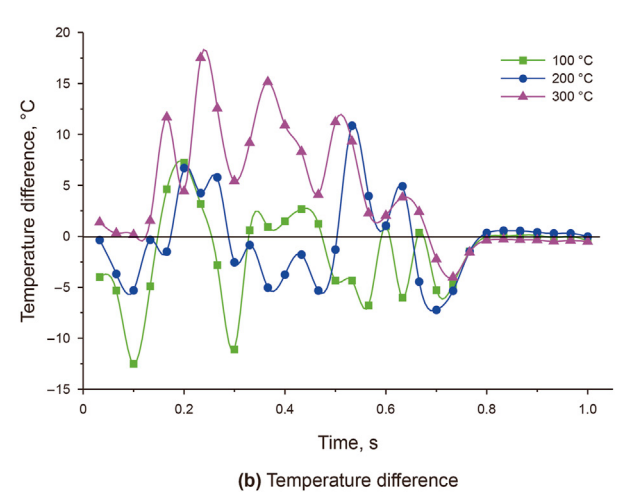


Fig. 12. The temperature variation with time increase while PDC cutter cutting granite.

investigated, as shown in Fig. 13(a). Unlike granite, all the groups of heated sandstone samples have a relatively higher temperature rise than the group of unheated samples. There is an approximately 1.08–2.57 °C gap of temperature rise between the heated rock cutting and unheated rock cutting. At the initial stage of cutting, it is noted that the temperature rise of the high temperature treated rock increases at a higher rate compared to the unheated rock. Moreover, during the cutting process, a steady temperature variation can be observed in both rock samples with and without high temperature treatment. However, there is no discernible difference in temperature rise between 100, 200, and 300 °C. The temperature difference is also acquired by subtracting the temperature rise of the room temperature group. As shown in Fig. 13(b), the results show that the temperature difference increases rapidly at the early cutting stage and decreases quickly at the end stage of cutting. However, it can be observed that the maximum temperature difference for each group's PDC cutter is not significant. From the temperature rise and temperature difference of the PDC cutter, it can be concluded that there is a critical temperature range from room temperature to 100 °C, which efficiently enhances the heat generation of the PDC cutter when cutting sandstone.

The results of the temperature variations of the granite and sandstone samples imply that the average temperature rise when cutting granite is substantially greater than that when cutting sandstone. Besides, there is a critical temperature range at which the temperature rise changes sharply when each rock type is cut by the PDC cutter. This critical temperature range is dependent on the rock properties after high temperature treatment.

(3) Temperature field of PDC cutter

Fig. 14 shows the temperature graph that is recorded by the thermal infrared imager. When the treatment temperature changes from 9 to 200 °C, the maximum temperature of the PDC cutter shows no significant difference. However, as the treatment temperature of granite rises to 300 °C, the highest temperature value of the PDC cutter is observed in the four groups. The maximum temperature of the PDC cutter reaches 47.6 °C, almost 10 °C higher than that in other conditions. Similarly, the maximum temperature of sandstone cutting also varies from 13.01 to 13.59 °C when the treatment temperature increases from 9 to 300 °C. Thus, the maximum temperature of the PDC cutter while cutting high temperature treated rock is higher than that low temperature treated rock. Compared with granite cutting, the maximum temperature of

sandstone cutting is relatively lower. The four images of sandstone cutting indicate that the critical treatment temperature is approximately in the range of $9{-}100~^{\circ}\text{C}$.

3.4. Temperature effect on rock debris

According to the images taken by the high-speed camera, there is much debris when cutting the heated specimen using the PDC cutter (see Fig. 15(a–c)). Some huge debris has been removed from the granite on the front side. Comparing the cutting debris at different treatment temperatures, it was discovered that the amount of large cutting debris increased as the treatment temperature went up. More and more large cutting debris was detected (see Fig. 15(b–d)) for both the granite cutting and the sandstone cutting. However, compared to granite debris, flake-like debris is more prevalent in sandstone debris. Meanwhile, the size of sandstone debris is generally larger than that of granite debris.

To quantitatively evaluate the cutting debris, the maximum geometric size of the cutting debris in each group was measured. Table 3 shows the maximum length and width of debris at different treated temperatures. The results indicate that the maximum length of the cutting debris from heated granite and sandstone is larger than that from unheated granite and sandstone, respectively. In particular, the maximum length of cutting debris from heated sandstone, which ranges from 6 to 8 mm, is larger than that of unheated sandstone. This is due to the decrease in the Young's modulus of the granite and sandstone as the temperature increases to 300 °C. Consequently, during the cutting process with PDC cutters, larger and more numerous cracks are generated, ultimately leading to an increase in the size of the rock debris. Compared to the maximum length of cutting debris for granite and sandstone, it can be seen that the maximum length of cutting debris is the same at room temperature for both granite and sandstone. However, when the treatment temperature rises, the maximum length of sandstone cutting debris increases dramatically. The maximum width of granite cutting debris is reduced with increasing treatment temperature, but the maximum width of the sandstone cutting debris rises slightly. The gap of the maximum width between the heated rock and unheated rock is not huge. Based on the geometrical scale of the debris, it can be observed that the size variation of sandstone debris is more pronounced compared to granite. It can be found that the increasing treatment temperature changes the mechanical properties of the sandstone more obviously than those of the granite, leading to a stronger generation of

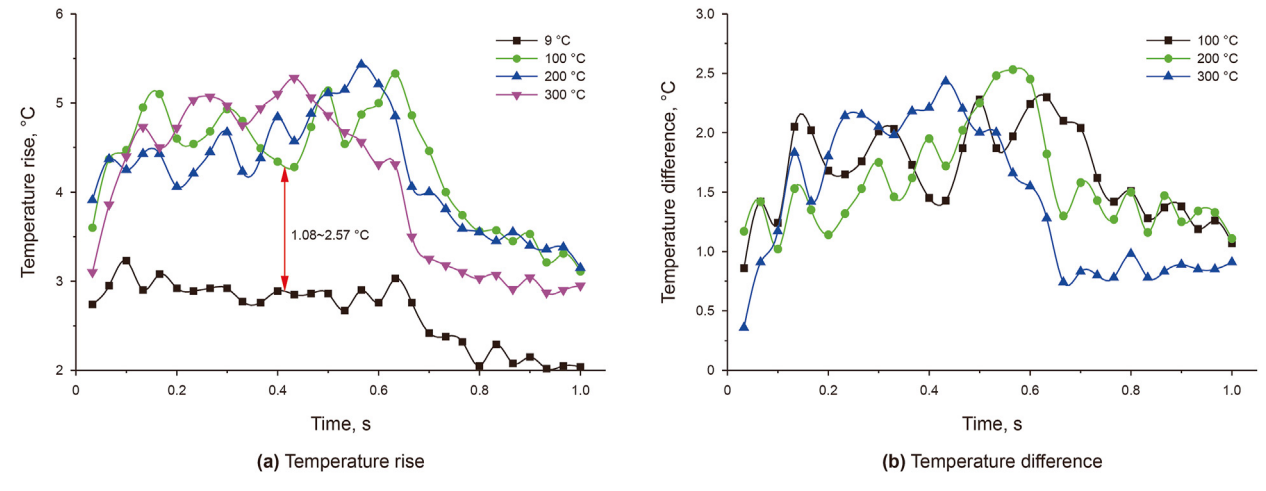


Fig. 13. The temperature variation with time increase while PDC cutter cutting sandstone.

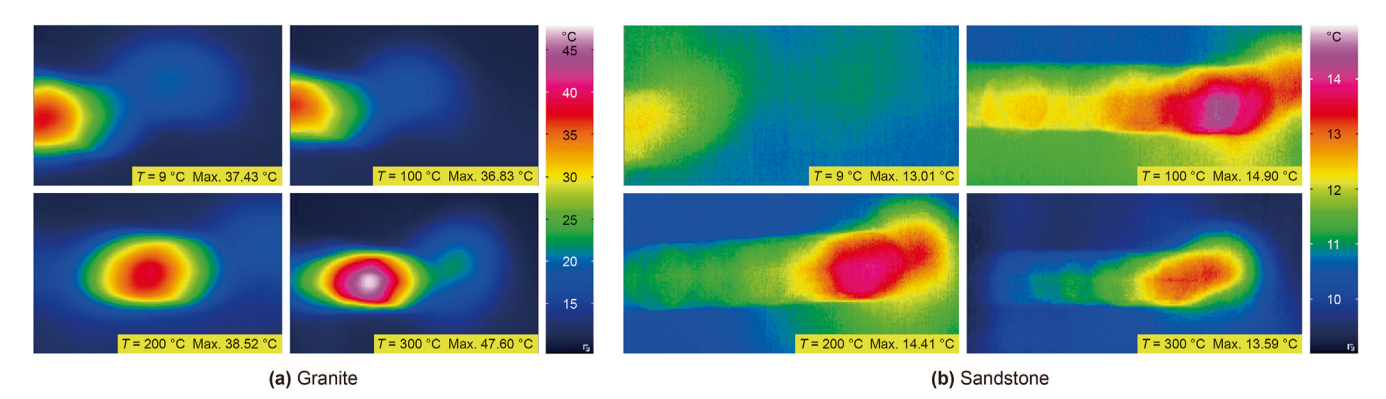


Fig. 14. Temperature field of PDC cutting.

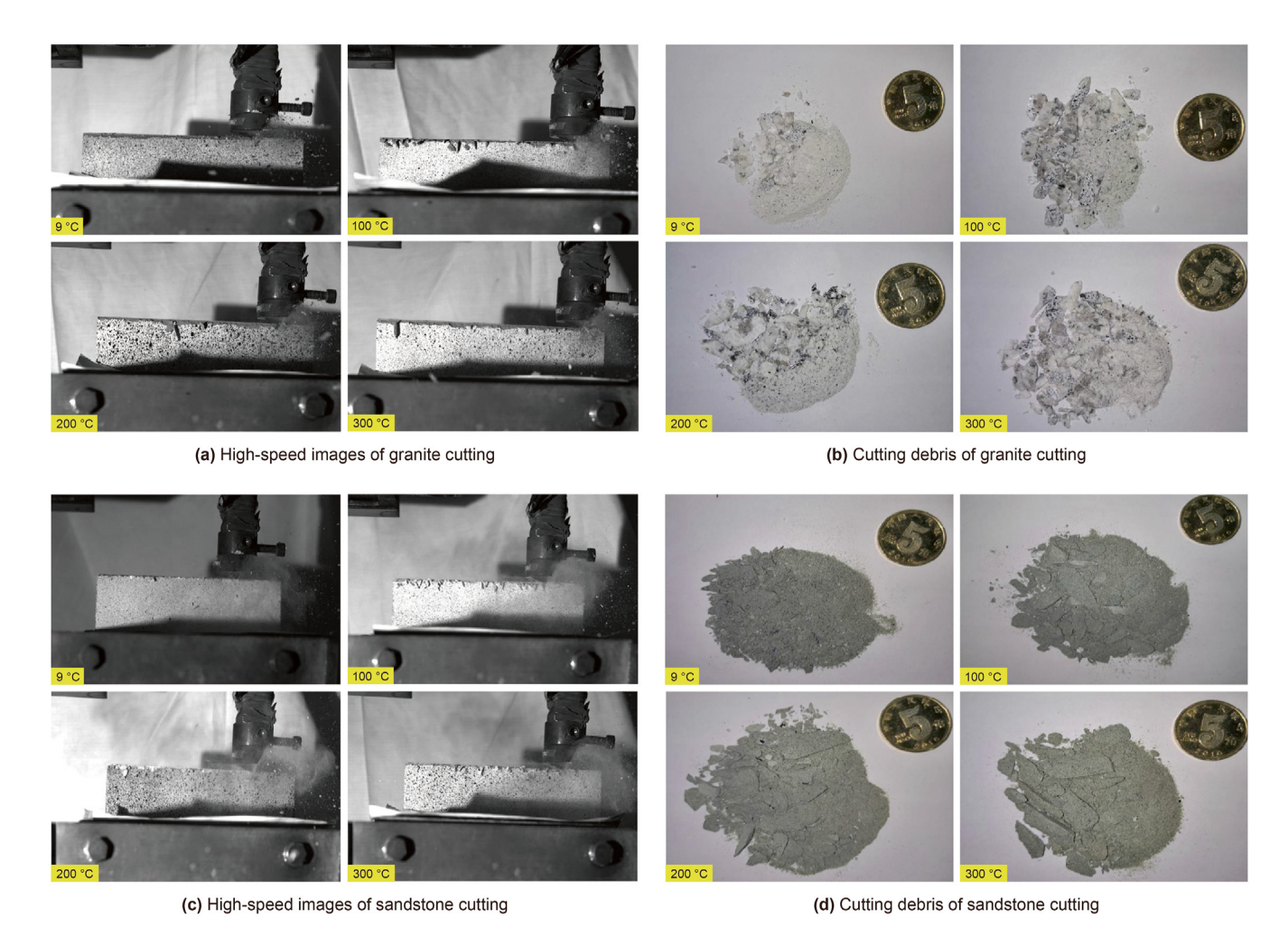


Fig. 15. Schematic diagram of cutting process and its cutting debris.

Table 3Maximum geometric size of the cutting debris at different treatment temperatures.

Treatment temperature, °C	Maximum length, mm		Maximum width, mm	
	Granite	Sandstone	Granite	Sandstone
9	14	14	7	6
100	15	23	4	8
200	15	20	6	8
300	15	21	6	7

large cutting debris.

3.5. Cutting area effect on cutter temperature

To comprehensively investigate the roles of cutter friction and rock deformation in heat generation, a comparative experiment was designed, utilizing both half-cutter and whole-cutter to cut the heat-treated rock. As shown in Fig. 16, all parameters of interest, including rake angle, cutting speed, and cutter diameter, are identical except for the cutting depth. Since the cutting force,

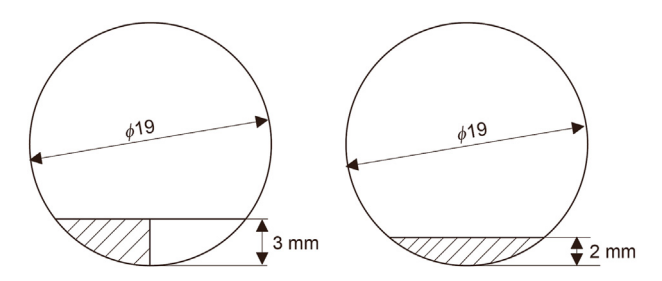


Fig. 16. The schematic graph of half-cutter cutting and whole-cutter cutting.

temperature rise, and thermal images of the half-cutter cutting have been previously presented, the results of the whole-cutter cutting are shown as follows.

As can be seen from Fig. 17, when the treatment temperature is lower than 100 °C, the increasing rate and maximum value of the force curve are approximately the same for both axial and tangential forces. With the increase in treatment temperature, the increasing rate and maximum value of the force curves reduce greatly (see Fig. 17(a and b)). Compared to the cutting results of other heated rock samples, the axial and tangential forces exhibit a rapid reduction trend. The average values of the axial and tangential forces grow smoothly with increasing treatment temperature and are ultimately reduced when the treatment temperature exceeds 200 °C (see Fig. 17(c)). Compared with the results of

half-cutter cutting in Fig. 17(d), it is found that the average axial force and tangential force of whole-cutter cutting are 3 and 3.4 times that of half-cutter cutting, respectively; even the contact area of whole-cutter is 1.67 times that of half-cutter.

The temperature variation of the PDC cutter was measured when the thick rock sample was cut. As shown in Fig. 18(a), the curves of temperature rise show a smoothly growing trend with cutting time rise. At 0.666 s, the temperature rise starts to decline because of the reduction of the PDC cutter cutting speed. Fig. 18(a) also shows that there is not much difference in temperature rise between the unheated and heated rock cuttings when using the whole-cutter. However, the temperature difference fluctuated apparently with increasing cutting time. The heated rock cutting at 200 °C has the highest temperature difference, clearly indicating that the granite heating to 200 °C would significantly affect the temperature rise of the PDC cutter. It is revealed that the fluctuation in temperature difference represents the periodic interaction between heat generation and heat dissipation during cutting with the PDC cutter.

By using the whole-cutter, the maximum temperature of the PDC cutter is much higher than that of the half-cutter (see Fig. 19). The thermal images of the sandstone cutting demonstrate that the maximum temperature increased from 17.93 to 20.52 °C when the treatment temperature of the sandstone varied from 9 to 200 °C before it declines slightly to 18.51 °C. Moreover, the maximum temperature of the whole-cutter cutting is 5-6 °C higher than that of the half-cutter cutting. This indicates that the highest maximum

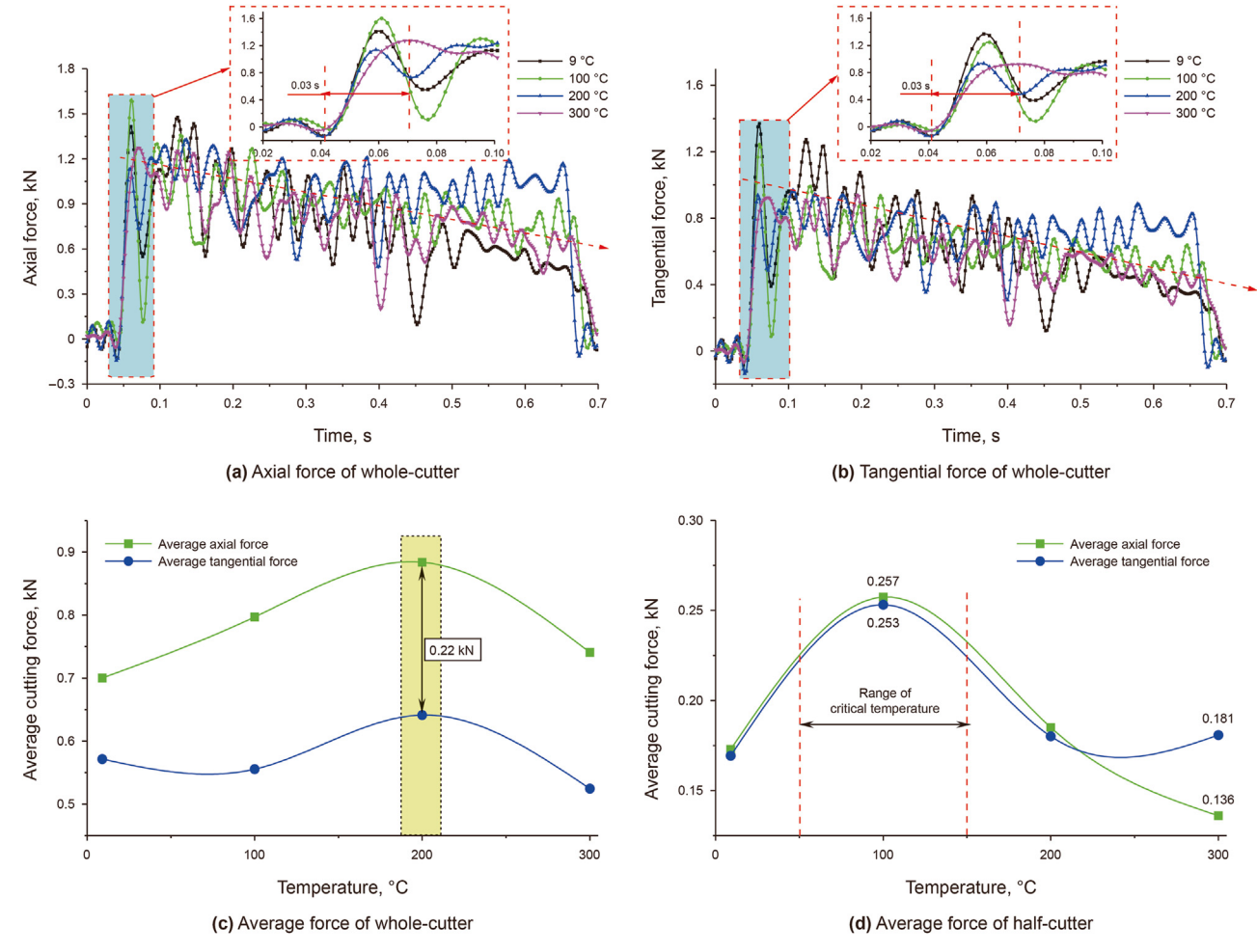


Fig. 17. The measured force of whole-cutter cutting

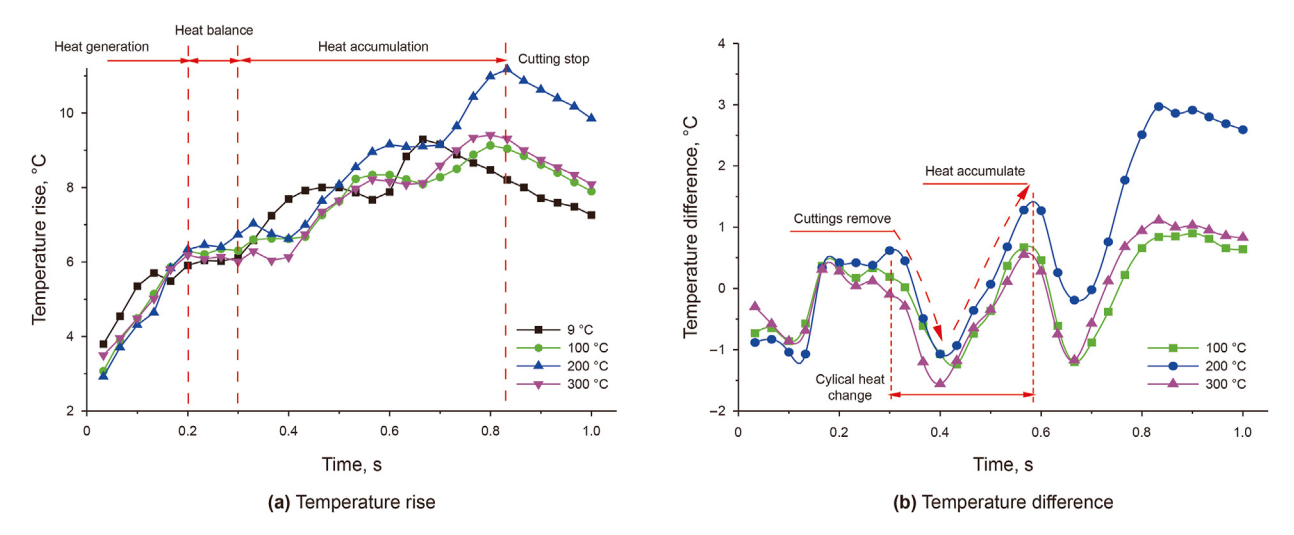


Fig. 18. The temperature variation of whole-cutter cutting.

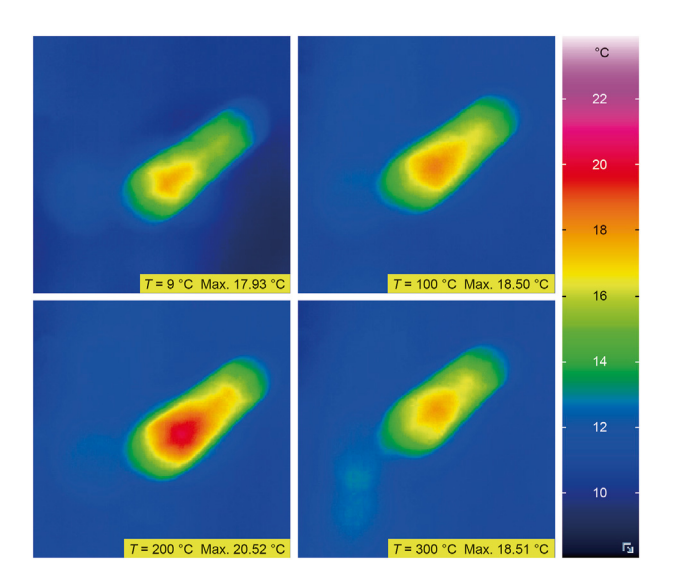


Fig. 19. The thermal images of whole-cutter cutting.

temperature occurs at a treatment temperature of 200 °C. As shown in Fig. 20, the cutting size of the whole-cutter cutting is smaller than that of the half-cutter cutting. Besides, it is found that by using whole-cutter, the cutting size of un-heated sandstone is larger than that of heated sandstone (see Fig. 20). In addition, it is clear that the whole-cutter cutting produce much smaller block cutting debris, but the half-cutter cutting create much more plate-like debris. The whole-cutter cutting provides a larger contact area and more uniform stress distribution, which promotes plastic deformation of the rock, resulting in a higher proportion of plastic failure. This explains why whole-cutter cutting produces smaller rock chips compared to half-cutter cutting.

4. Discussion

4.1. Coefficient of friction and heat generation

The heat generated during rock sample cutting is mostly caused by the deformation of the cutting debris and the contact friction between the PDC cutter and the rock. So, the Coefficient of Friction (COF), $K_{\rm f}$, is used to represent the contact friction, which is defined as:



Fig. 20. The cutting chips of whole-cutter cutting.

$$K_{\rm f} = F_{\rm N/F_{\rm t}} \tag{2}$$

where K_f is the friction coefficient between the rock and the cutter; F_N is the axial force, and F_t is a tangential force that is also named as cutting force in this article.

As shown in Fig. 21(a and b), K_f of different rocks is compared. At the beginning of PDC cutting, the K_f quickly drops and sharply rises to its maximum value. It means the contact friction between the PDC cutter and rock is extremely varied as the cutter starts cutting. Comparing K_f values of granite and sandstone, it is found that the granite sample treated at 300 °C has the lowest K_f value of 0.24. In contrast, the sandstone sample treated at 200 °C has the lowest K_f value. This implies a strong relationship between the treatment temperature and K_f .

Compared K_f of cutting process by the half-cutter and whole-cutter (Fig. 21(b and c)), K_f of the whole-cutter cutting is found to be less than that of half-cutter cutting, suggesting that the friction is decreased with increasing treated temperature when using the whole-cutter. Thus, the increase in heat generation of whole-cutter cutting would be mainly own to the rock deformation. The average K_f of each curve in Fig. 21(a–c) is calculated and shown in Fig. 21(d).

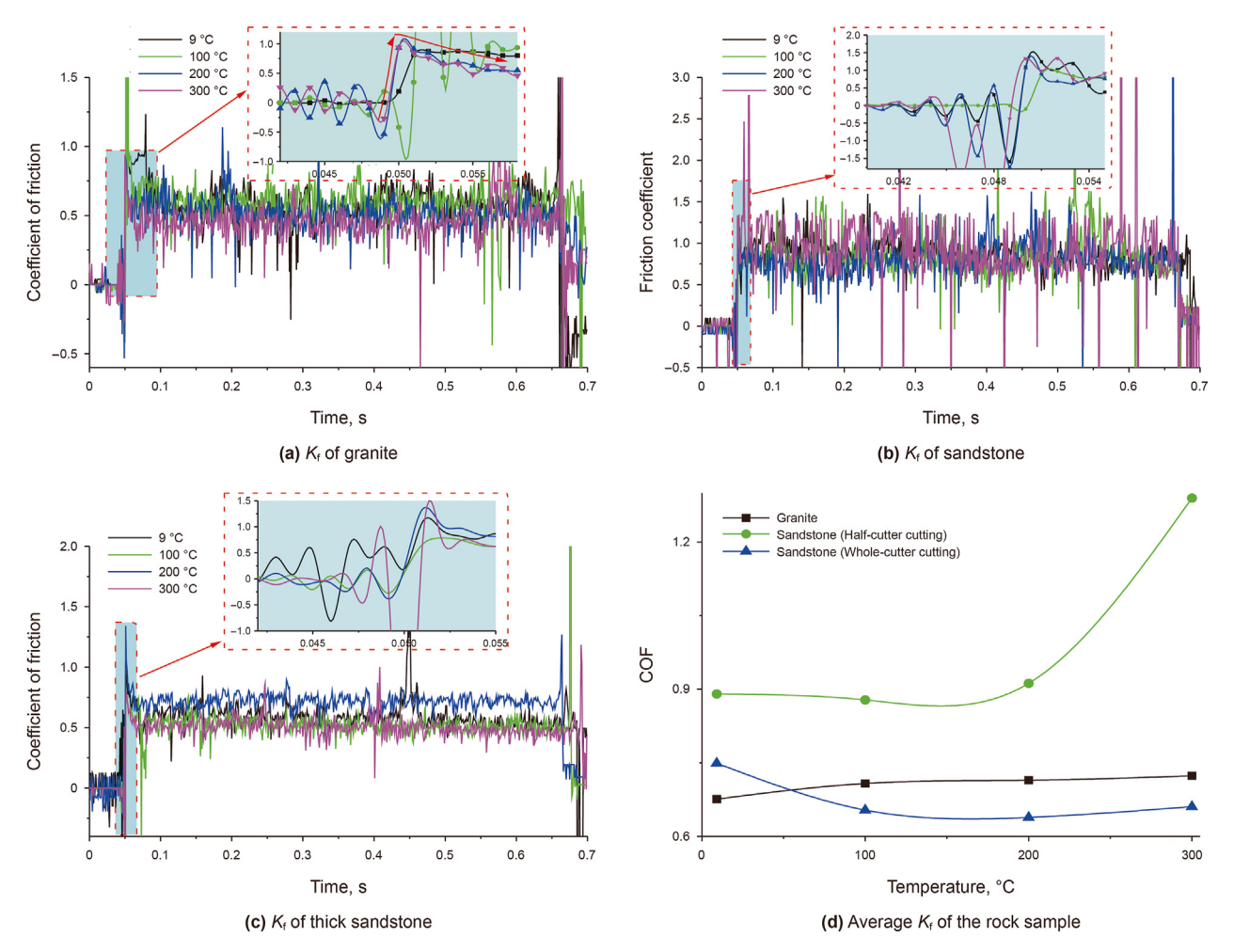


Fig. 21. K_f of the rock sample.

Clearly, the average K_f value of sandstone cutting remains steady when the treatment temperature is below 200 °C, and then sharply increases when the treatment temperature exceeds 200 °C. For the granite cutting by half-cutter, K_f smoothly grows from 0.89 to 0.91 when the treatment temperature changes from 9 to 200 °C, and finally becomes stable at a treatment temperature of 300 °C. This implies that for the half-cutter cutting, the heat generation from friction plays a more and more important role with the increasing treatment temperature. Otherwise, the K_f of whole-cutter cutting reduces from 0.75 to 0.66 when the treatment temperature of sandstone is increased from 9 to 300 °C. This K_f is not only lower than that of the half-cutter cutting but also shows an opposing changing trend, which suggests that the whole-cutter cutting makes a slightly negative contribution to heat generation even when the rock is heated to over 200 °C. Thus, in conclusion, for bits designed for hot well drilling, increasing the cutter-rock contact area can significantly reduce heat generation from friction, but the cutting force and temperature rise increase significantly.

We noticed that the K_f is a key factor affecting heat generation, influencing the cutter temperature rise and rock temperature variation. Glowka (1989) proposed the heat generation model in which friction is responsible for the temperature rise. This model is used to calculate the cutter temperature variation, which is determined by a particular equation (Azar et al. 2007; Glowka, 1989):

$$T_{\rm c} = T_{\rm f} + \frac{K_{\rm f} F_{\rm n} v_{\rm c}}{A_{\rm w}} \left(1 + \frac{3\pi}{4} f K_{\rm hf} \sqrt{\frac{v_{\rm c}}{\alpha_{\rm f} L_{\rm w}}} \right)^{-1} \tag{3}$$

where

 $T_{\rm c}$ and $T_{\rm f}$ are the cutter and fluid temperature, respectively, T; $K_{\rm f}$ is the friction coefficient between the rock and the cutter, constant;

 v_c is the cutter speed, m/s;

 $L_{\rm w}$ is cutter cutting edge length parallel to cutting direction, m; $A_{\rm w}$, cutter-rock interface area in contact with the rock, m²;

 F_n is the axial force on the cutter, N;

f is the thermal response function, constant;

 $K_{\rm hf}$, $\alpha_{\rm f}$ are the rock thermal conductivity and diffusivity, respectively.

In our experiments, v_c , L_w , and A_w are known and are 0.46 m/s, 3×10^{-3} m, and 3×10^{-6} m², respectively. The F_n can be obtained from Sections 3.2 and 3.5, and K_f has been calculated by Eq. (2). The temperature rise (ΔT) can be obtained through the observation of thermal infrared imaging. Combining Eq. (3), Glowka's equation as a function of the parameters can be written as follows:

$$\Delta T = T_{\rm c} - T_{\rm f} = \frac{K_{\rm f} F_{\rm n} v_{\rm c}}{A_{\rm W} \left(1 + \frac{3\pi}{4} f K_{\rm hf} \sqrt{\frac{v_{\rm c}}{\alpha_{\rm f} L_{\rm w}}} \right)} \tag{4}$$

Here v_c , L_w and A_w are constant parameters, and F_n and K_f are measured by sensors and Eq. (2). f, K_{hf} and α_f all vary with the temperature rising in the cutting process, which cannot be easily measured. Then, Eq. (4) could be written as:

$$\frac{fK_{\rm hf}}{\sqrt{\alpha_{\rm f}}} = \frac{4}{3\pi} \left(\frac{K_{\rm f} F_{\rm n} v_{\rm c}}{\Delta T A_{\rm w}} - 1 \right) \sqrt{\frac{L_{\rm w}}{v_{\rm c}}} \tag{5}$$

To describe the heat transfer and conversion in the cutting process, a new parameter η is defined as:

$$\eta = \frac{fK_{\rm hf}}{\sqrt{\alpha_{\rm f}}} \tag{6}$$

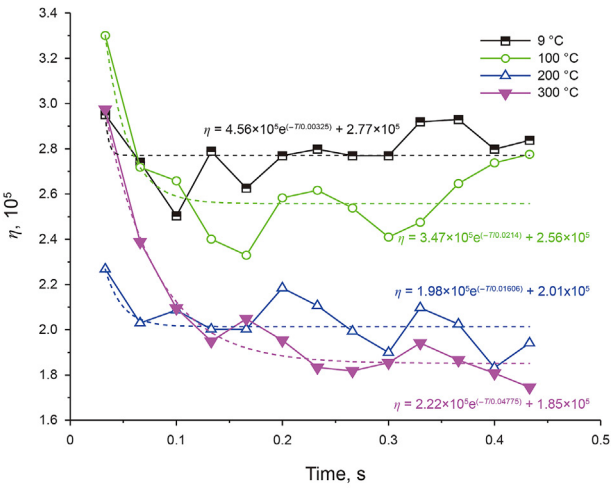
Combining Eqs. (5) and (6), results in the expression for the thermal converted function at the cutter-rock interface, η as:

$$\eta = \frac{4}{3\pi} \left(\frac{K_f F_n v_c}{\Delta T A_w} - 1 \right) \sqrt{\frac{L_w}{v_c}} \tag{7}$$

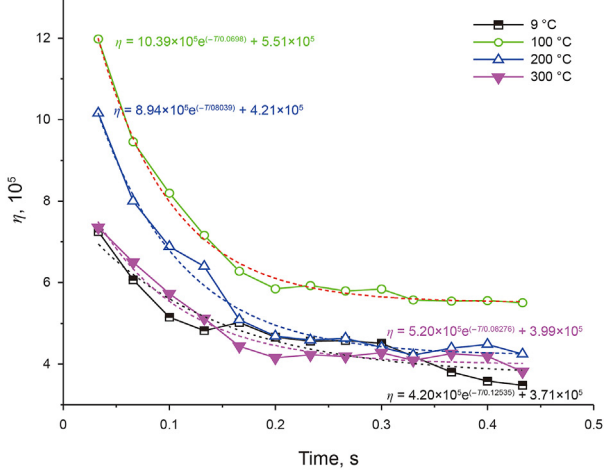
On the one hand, it is noticed that the new parameter η , is related to frictional heating at the cutter-rock interfaces according to Eq. (7); on the other hand, it is also an index for evaluating the thermal response at the cutter-rock interface. Therefore, by using the new evaluation index, η , thermal responses of the three typical rock specimens during cutting are obtained and compared in Fig. 22.

This figure shows that n decreased rapidly during the time period of 0-0.3 s, then gradually stabilized. However, the cutting edge length of the PDC cutter parallel to the cutting direction can affect the decreasing trend and the time required for η to reach a steady state. The comparison between Fig. 22(a) and (b) shows that there is a long time of heat conversion and transmission when the cutting edge length is larger. Since the cutting edge length for the thick specimen is double that of the thin specimen (see Fig. 16), it leads to greater frictional heat generation and a longer heat transfer time. That's the main reason why η of thick specimen reach the steady value at 0.3 s and the thin sandstone gets the stable η at 0.1 s. Rock types also play a vital role in the heat generation and transmission between the cutter and rock. To this end, the η values of sandstone and granite (see Fig. 22(a) and (c)) are compared. The results indicate that the granite specimen exhibits a more sharply declining trend than the sandstone specimen. According to the defined Eq. (7), we know that the heat generation and transmission are calculated by the rock thermal conductivity and diffusivity. Sun et al. (2016) reported in their study that the thermal conductivity of the sandstone reduced from 2.21 to 1.41 W/(m·k) when the treatment temperature changed from room temperature to 300 °C. In Chen's study (Chen et al., 2016) the thermal conductivity of granite reduced from 2.8 to 2.3 W/($m \cdot k$), which is higher than that of the sandstone in Sun's results (Sun et al., 2016). We also found that the thermal diffusivity of granite varied in the range of 12×10^{-3} to $5.8 \times 10^{-3} \text{ cm}^2 \text{ s}^{-1}$ as the treatment temperature rose from 300 to 600 °C, which is smaller than that of sandstone, which dropped from 18×10^{-3} to 8×10^{-3} cm² s⁻¹ over the same temperature range (Hanley et al., 1978). Sometimes, the thermal diffusivity of granite could even be 30×10^{-3} cm² s⁻¹ (Sun et al., 2016). The above examples indicate that granite has a larger ratio of thermal conductivity to thermal diffusivity than sandstone. That is the main reason why η of thin granite specimen is mostly larger than that of thin sandstone specimen. The variation of η also supports the idea that the capacity of heat generation and transmission would change with the temperature rise at the cutter-rock interface.

In addition, after fitting the measured curve, an exponential curve was obtained. It can be seen that the stable value of thin



(a) Thin sandstone



(b) Thick sandstone

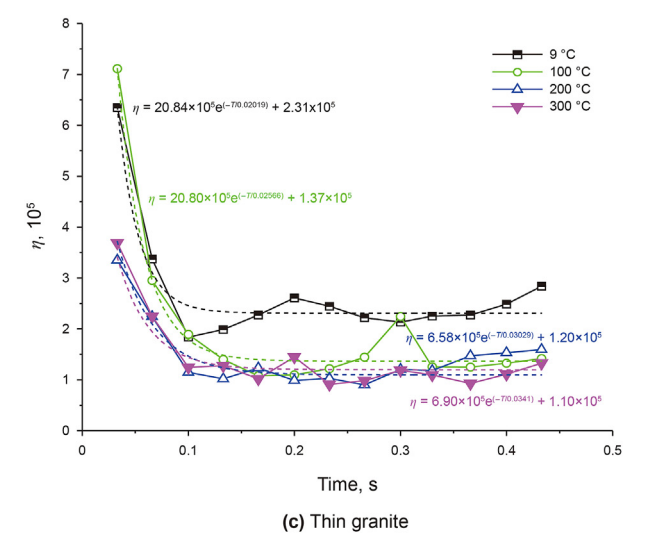


Fig. 22. Thermal response of the three typical rock specimens during cutting.

sandstone (Fig. 22(a)) increased from 1.85×10^5 to 2.27×10^5 when the treatment temperature rose from 9 to 300 °C. However, a decreasing trend is observed for the thin granite specimens when the treatment temperature rises to 300 °C, revealing that there are different thermal heat generation and transmission capacities

between granite and sandstone at the cutter-rock interface within the experimental range of treatment temperatures.

4.2. Correlation of rock properties and cutting force post-thermal damage

In terms of the mechanical properties of high-temperature-treated rock, we also noticed that the rock properties varied correspondingly with the treatment temperature, as shown in Table 1 and Fig. 5. The high temperature treatment affects the mechanical properties of sandstone and granite, leading to different rock-breaking performances. Several researchers, such as Qin et al. (2020), Chen et al. (2012), and Zhang et al. (2021), have successfully defined rock thermal damage based on the reduction of rock properties to evaluate the influence of high-temperature treatment on rock mechanical properties. To consider the existence of a critical temperature, Chen et al. (2012) proposed two polynomials to describe the effect of temperature on Young's modulus:

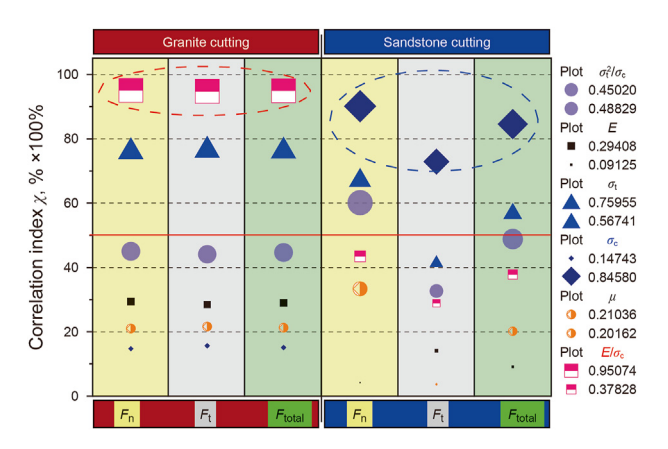


Fig. 23. Correlation index analysis for all evaluation parameters.

The values of the Correl Index Function χ (F_i , X) versus temper-

$$\frac{E(T)}{E_0} = \begin{cases}
0.2 \times \left(\frac{T}{1000}\right)^2 - 0.3\left(\frac{T}{1000}\right) + 1.0052 & (20 \,^{\circ}C \le T \le 400 \,^{\circ}C) \\
2 \times \left(\frac{T}{1000}\right)^2 - 4.8\left(\frac{T}{1000}\right) + 2.4795 & (400 \,^{\circ}C \le T \le 1000 \,^{\circ}C)
\end{cases}$$
(8)

According to the findings of this study, there is a relationship between rock property and cutting force after thermal damage, which is related to the heated treatment temperature as shown in Eq. (8). Firstly, a correlation analysis between the rock property and cutting force was conducted, see Fig. 23. The $\sigma_{\rm t}^2/\sigma_{\rm c}$ (Li et al., 2018; Evans et al., 1965), E, $\sigma_{\rm t}$, $\sigma_{\rm c}$, μ and $E/\sigma_{\rm c}$ (Rostamsowlat et al., 2019) were previously selected to calculate the correlation index, as such an approach had been successfully applied to evaluate rockbreaking. The correlation index formula is shown as the following equation:

$$Correl(F_i, X) = \frac{\sum (x - \overline{x})(F_i - \overline{F}_i)}{\sqrt{\sum (x - \overline{x})^2 \sum (F_i - \overline{F}_i)^2}}$$
(9)

where F_i denotes F_n , F_t and F_{total} , X is σ_t^2/σ_c , E, σ_t , σ_c , μ and E/σ_c .

ature for both sandstone and granite are plotted in Fig. 23. It is found that the cutting force (F_t) is highly correlated with σ_t^2/σ_c , E/σ_c and σ_t . The high correlation evaluated index indicates that the cutting force of the sandstone is highly related to σ_t^2/σ_c . But the granite cutting force of granite has a strong relationship with E/σ_c . It can also be seen that the former evaluation index σ_t^2/σ_c is more efficient for evaluating the cutting of granite, while E/σ_c is more appropriate for evaluating the cutting of sandstone.

Based on the correlation analysis, the cutting force is assumed to be a function of four factors, $\sigma_{\rm f}^2/\sigma_{\rm c}$, E, $\sigma_{\rm t}$, $\sigma_{\rm c}$ and $E/\sigma_{\rm c}$, respectively:

$$F_{t}(T) = f(E(T) / \sigma_{c}(T), \sigma_{c}(T), \sigma_{t}(T), \sigma_{t}^{2}(T) / \sigma_{c}(T))$$
(10)

 $F_{\rm t}(T)$ is believed to be a linear function consisting of four parts, eg. $\sigma_{\rm t}^2/\sigma_{\rm c}$, E, $\sigma_{\rm t}$, $\sigma_{\rm c}$ and $E/\sigma_{\rm c}$. Therefore, for each treatment temperature T ($T=9-300~{\rm ^{\circ}C}$), a linear function can be written as:

$$\begin{cases} F_{t}(T=9) = k_{1} \left(\frac{E}{\sigma_{c}}\right)_{T=9} + k_{2}(\sigma_{c})_{T=9} + k_{3}(\sigma_{t})_{T=9} + k_{4} \left(\frac{(\sigma_{t})^{2}}{\sigma_{c}}\right)_{T=9} \\ F_{t}(T=100) = k_{1} \left(\frac{E}{\sigma_{c}}\right)_{T=100} + k_{2}(\sigma_{c})_{T=100} + k_{3}(\sigma_{t})_{T=100} + k_{4} \left(\frac{(\sigma_{t})^{2}}{\sigma_{c}}\right)_{T=100} \\ F_{t}(T=200) = k_{1} \left(\frac{E}{\sigma_{c}}\right)_{T=200} + k_{2}(\sigma_{c})_{T=200} + k_{3}(\sigma_{t})_{T=200} + k_{4} \left(\frac{(\sigma_{t})^{2}}{\sigma_{c}}\right)_{T=200} \\ F_{t}(T=300) = k_{1} \left(\frac{E}{\sigma_{c}}\right)_{T=300} + k_{2}(\sigma_{c})_{T=300} + k_{3}(\sigma_{t})_{T=300} + k_{4} \left(\frac{(\sigma_{t})^{2}}{\sigma_{c}}\right)_{T=300} \end{cases}$$

where k_1 , k_2 , k_3 and k_4 are the constant parameters, and the constant array of [K] could be expressed as the following equation:

$$[K] = [k_1 \quad k_2 \quad k_3 \quad k_4] \tag{12}$$

Eqs. (11) and (12) yield

$$[F_t] = [K] \left[\begin{bmatrix} \frac{E}{\sigma_c} \end{bmatrix} \quad [\sigma_c] \quad [\sigma_t] \quad \left[\frac{(\sigma_t)^2}{\sigma_c} \right] \right]$$
 (13)

By using the Python code, the constant parameters of the cutting force at the temperature range from 9 to 300 °C could be calculated

$$[K]_{\text{sandstone}} = [2.6315 -0.1288 \ 2.6064 -13.2931]$$
 (14)

$$[K]_{Granite} = [3.0270 \quad -0.1707 \quad 5.9083 \quad -47.7354]$$
 (15)

Finally, this constructor function of Eq. (13) could be used to illustrate the relationship between the rock properties and the cutting force at different treatment temperatures.

5. Conclusions

In this study, an experiment is designed considering the multimeasuring method, including the cutting force sensor, high-speed photography and thermal infrared imager. The cutting force, temperature rise and cutting size are discussed in detail. Moreover, a comparison between whole-cutter cutting and half-cutter cutting is conducted. Finally, a new evaluation parameter, η , related to frictional heat generation, has been proposed to better reflect the thermal response during the rock cutting process. This research provides valuable insights into rock breakage and heat generation during PDC cutting in HDR well drilling. The main conclusions are as follows.

- (1) The comparison of the average cutting force between granite cutting and sandstone cutting indicates that the average cutting force of granite ranges from 3 to 5 times the average cutting force of the sandstone sample. There are different critical temperatures for granite and sandstone, respectively, at which the cutting force and temperature rise vary significantly. The cutting force of sandstone will significantly decrease at approximately 100 °C, while the cutting temperature rise will significantly increase at 75-150 °C. The cutting force of granite will decrease initially as the treatment temperature increases, then heavily increases after 100-200 °C, and the cutting temperature rise will significantly increase after 200-300 °C.
- Combining the variations in maximum length and width, it is found that the large debris increases significantly among the granite and sandstone debris with increasing treatment temperature. In the larger rock debris, the sandstone fragments exhibit a more flaky structure. Additionally, the debris generated by whole-cutter cutting is smaller in size compared to that produced by half-cutter cutting, and the cutting temperature is also higher.
- It is noticed that the newly defined evaluation index (η) is related to frictional heating at the cutter-rock interfaces. The η of thin granite specimen is mostly larger than the η of thin sandstone specimen. The stable value of thin sandstone increases from 1.85×10^5 to 2.27×10^5 when the treatment temperature rises from 9 to 300 °C. However, a reduction trend is observed for the thin granite specimen when the treatment temperature rises to 300 °C. There is different

- thermal heat and transmission capacity between granite and sandstone at the cutter-rock interface, while the treatment temperature rises from 9 to 300 °C.
- (4) The cutting force (F_t) is highly correlated with σ_t^2/σ_c , E/σ_c and $\sigma_{\rm f}$. The cutting force of sandstone is greatly related to $\sigma_{\rm f}^2/\sigma_{\rm c}$ while the E/σ_c has a strong relationship with granite cutting force. The former evaluation index of $\sigma_{\rm t}^2/\sigma_{\rm c}$ is more efficient for evaluating granite cutting, while E/σ_c is more appropriate for evaluating sandstone cutting.

CRediT authorship contribution statement

Can Cai: Writing – original draft, Visualization, Validation, Methodology, Funding acquisition, Data curation, Conceptualization. Wen-Yang Cao: Writing - review & editing, Resources, Data curation. Xian-Peng Yang: Writing - review & editing, Validation, Methodology. Quan-Gong Xie: Validation, Resources. Bang-Run Li: Validation, Investigation. Zheng-Bo Tan: Software, Investigation. Chun-Liang Zhang: Visualization. Chi Peng: Validation. Hao Chen: Visualization. Yu-Long Zhao: Validation.

Declaration of interest statement

We declare that there is no conflict of interests regarding the publication of this paper. All authors have read the manuscript and approved to submit to your journal. The current manuscript has not been sent elsewhere for evaluation or presentation.

Acknowledgments

This work was supported by the National Natural Science Foundation of China (Grant No. 52004236), the Key Program of National Natural Science Foundation of China (Grant No. 52234003), Sichuan Provincial Returned Scholars' Scientific and Technological Activities Merit-based Funding Programs (Grant No. 2023016), Open project of the International Joint Research Center for Deep Earth Drilling and Deep Earth Resources Development of the Ministry of Science and Technology (Grant No. DEDRD-2023-06), the National Natural Science Foundation of China Outstanding Youth Science Fund Program (Grant No. 52222402). We appreciate for the contribution of the strength testing by Mei Yang. We also thank for the support from Chengdu iDrill Energy Technology Co., Ltd.

References

Agostini, C.E., Sampaio, M.A., 2020. Probabilistic neural network with Bayesianbased, spectral torque imaging and deep convolutional autoencoder for PDC bit wear monitoring. J. Petrol. Sci. Eng. 193, 107434. https://doi.org/10.1016/ j.petrol.2020.107434

Akbari, B., Miska, S., 2016. The effects of chamfer and back rake angle on PDC cutters friction. J. Nat. Gas Sci. Eng. 35, 347-353. https://doi.org/10.1016/ j.jngse.2016.08.043.

Akbari, B., 2014. PDC Cutter-Rock Interaction-Experiments and Modeling. PhD Thesis. The University of Tulsa.

Akbari, B., 2011. Polycrystalline Diamond Compact Bit-Rock Interaction. Master Thesis, Memorial University of Newfoundland, http://research.library.mun.ca/ id/eprint/10061

Apple, F.C., Wilson, C.C., Lakshman, I., 1993. Measurement of forces, temperatures and wear of PDC cutters in rock cutting. Wear 169 (1), 9-24. https://doi.org/ 10.1016/0043-1648(93)90386-Z.

Azar, J.J., Samuel, G.R., 2007. Drill bit mechanic. Drilling Engineering. PennWell

Books, Tulsa, Oklahoma, pp. 277–317. Cai, C., Zhang, P., Xie, S., et al., 2023. Rock breakage and temperature variation of naturally worn PDC tooth during cutting of hard rock and soft rock. Geoenergy and Engineering 229, 212042. https://doi.org/10.1016/ j.geoen.2023.212042.

Che, D., Ehmann, K., Cao, J., 2015. Analytical modeling of heat transfer in polycrystalline diamond compact cutters in rock turning processes. J. Manuf. Sci.

- Eng. 137 (3), 031005. https://doi.org/10.1115/1.4029653.
- Che, D., Zhang, W., Ehmann, K., 2017. Chip formation and force responses in linear rock cutting: an experimental study. J. Manuf. Sci. Eng. 139 (1), 011011. https:// doi.org/10.1115/1.4033905.
- Cheatham Jr., J.B., Daniels, W.H., 1979. A study of factors influencing the drillability of shales: single-cutter experiments with STRATAPAX (T) drill blanks. J. Energy Resour. Technol. 101 (3), 189–195. https://doi.org/10.1115/1.3446918.
- Chen, S., Yang, C., Wang, G., 2017. Evolution of thermal damage and permeability of Beishan granite. Appl. Therm. Eng. 110, 1533—1542. https://doi.org/10.1016/ j.applthermaleng.2016.09.075.
- Chen, Y.L., Ni, J., Shao, W., et al., 2012. Experimental study on the influence of temperature on the mechanical properties of granite under uni-axial compression and fatigue loading. Int. J. Rock Mech. Min. Sci. 56, 62–66. https://doi.org/10.1016/j.ijrmms.2012.07.026.
- Chen, Z.M., Wu, X., Wang, H.W., et al., 2016. Research of thermal conductive characteristic of granite under high temperature. Sci. Technol. Eng. 16 (24), 193—197.
- Cheng, Z., Sheng, M., Li, G., et al., 2018. Imaging the formation process of cuttings: characteristics of cuttings and mechanical specific energy in single PDC cutter tests. J. Petrol. Sci. Eng. 171, 854–862. https://doi.org/10.1016/j.petrol.2018.07.083.
- Cirimello, P., Otegui, J.L., Sanchez, J.M., et al., 2018. Oil well drill bit failure during pull out: redesign to reduce its consequences. Eng. Fail. Anal. 83, 75–87. https://doi.org/10.1016/j.engfailanal.2017.09.020.
- Deng, Z.H., Pan, Z., Wu, Q.P., et al., 2011. Research on finite element simulation and experiment of temperature field in surface cutting used a new PDC cutter. Key Eng. Mater. 487, 366–370. https://doi.org/10.4028/www.scientific.net/KEM.487. 366.
- Detournay, E., Defourny, P., 1992. A phenomenological model for the drilling action of drag bits. Int. J. Rock Mech. Min. Sci. Geomech & Abstracts. Pergamon 29 (1), 13–23. https://doi.org/10.1016/0148-9062(92)91041-3.
- Ding, Q.L., Ju, F., Mao, X.B., et al., 2016. Experimental investigation of the mechanical behavior in unloading conditions of sandstone after high-temperature treatment. Rock Mech. Rock Eng. 49, 2641–2653. https://doi.org/10.1007/s00603-016-0944-x.
- Dougherty, P.S.M., Mpagazehe, J., Shelton, J., et al., 2015. Elucidating PDC rock cutting behavior in dry and aqueous conditions using tribometry. J. Petrol. Sci. Eng. 133, 529–542. https://doi.org/10.1016/j.petrol.2015.05.016.
- Evans, I., 1965. The force required to cut coal with blunt wedges. Int. J. Rock Mech. Min. Sci. Geomech & Abstracts. Pergamon 2 (1), 1–12. https://doi.org/10.1016/0148-9062(65)90018-5.
- Galarraga, C., Fierro, J.C., Riyami, A.I., et al., 2016. An unconventional fixed cutter cutting structure layout to drill through hard, abrasive conglomerates in deep wells—a case study. Abu Dhabi International Petroleum Exhibition and Conference. SPE D011S012R001. https://doi.org/10.2118/182879-MS.
- Gautam, P.K., Verma, A.K., Jha, M.K., et al., 2016. Study of strain rate and thermal damage of Dholpur sandstone at elevated temperature. Rock Mech. Rock Eng. 49, 3805—3815. https://doi.org/10.1007/s00603-016-0965-5.
- Glowka, D.A., 1989. Use of single-cutter data in the analysis of PDC bit designs: part 1-development of a PDC cutting force model. J. Petrol. Technol. 41 (8), 797–849. https://doi.org/10.2118/15619-PA.
- Hanley, E.J., Dewitt, D.P., Roy, R.F., 1978. The thermal diffusivity of eight well-characterized rocks for the temperature range 300–1000 K. Eng. Geol. 12, 31–47. https://doi.org/10.1016/0013-7952(78)90003-0.
- Hu, J., Sun, Q., Pan, X., 2018. Variation of mechanical properties of granite after high-temperature treatment. Arabian J. Geosci. 11, 1–8. https://doi.org/10.1007/s12517-018-3395-8.
- Huang, K., Ai, Z., Yang, Y., et al., 2019. The improved rock breaking efficiency of an annular-groove PDC bit. J. Petrol. Sci. Eng. 172, 425–435. https://doi.org/ 10.1016/j.petrol.2018.09.079.
- Huang, Y.H., Yang, S.Q., Tian, W.L., et al., 2017. Physical and mechanical behavior of granite containing pre-existing holes after high temperature treatment. Arch. Civ. Mech. Eng. 17 (4), 912–925. https://doi.org/10.1016/j.acme.2017.03.007.
- Huang, Z.P., Zhang, Y., Wu, W.D., 2016. Analysis of mechanical and wave properties of heat-treated marble by water cooling. Rock Soil Mech. 37 (2), 367–375. https://doi.org/10.16285/j.rsm.2016.02.008.
- Li, W., Ling, X., Pu, H., 2020. Development of a cutting force model for a single PDC cutter based on the rock stress state. Rock Mech. Rock Eng. 53 (1), 185–200. https://doi.org/10.1007/s00603-019-01893-7.
- Li, X., Wang, S., Ge, S., et al., 2018. A theoretical model for estimating the peak cutting force of conical picks. Exp. Mech. 58, 709–720. https://doi.org/10.1007/s11340.017.0372.1
- Liu, W., Gao, K., 2017. Drilling technical difficulties and solutions in development of Hot dry Rock geothermal energy. Adv. Pet. Explor. Dev 13, 63–69. https:// doi.org/10.3968/9456.

Liu, W., Zhu, X., 2019. Experimental study of the force response and chip formation in rock cutting. Arabian J. Geosci. 12 (15), 457. https://doi.org/10.1007/s12517-019-4585-8.

- Pessier, R., Damschen, M., 2011. Hybrid bits offer distinct advantages in selected roller-cone and PDC-bit applications. SPE Drill. Complet. 26 (1), 96–103. https:// doi.org/10.2118/128741-PA.
- Prakash, V., Appl, F.C., 1989. Temperature distribution in synthetic diamond cutters during orthogonal rock cutting. SPE Drill. Eng. 4 (2), 137–143. https://doi.org/10.2118/17268-PA
- Qin, Y., Tian, H., Xu, N.X., et al., 2020. Physical and mechanical properties of granite after high-temperature treatment. Rock Mech. Rock Eng. 53, 305–322. https://doi.org/10.1007/s00603-019-01919-0.
- Richard, T., Coudyzer, C., Desmette, S., 2010. Influence of groove geometry and cutter inclination in rock cutting. ARMA US Rock Mechanics/Geomechanics Symposium, pp. 10–429.
- Rostamsowlat, I., Richard, T., Evans, B., 2019. Experimental investigation on the effect of wear flat inclination on the cutting response of a blunt tool in rock cutting. Acta Geotechnica 14, 519–534. https://doi.org/10.1007/s11440-018-0674-1
- Sha, S., Rong, G., Tan, J., et al., 2020. Tensile strength and brittleness of sandstone and granite after high-temperature treatment: a review. Arabian J. Geosci. 13, 1–13. https://doi.org/10.1007/s12517-020-05647-6.
- Shi, Z.M., 2006. Testing and Analysis Cutting Force of PDC Cutters. PhD Thesis. Southwest Petroleum University.
- Sun, Q., Lü, C., Cao, L., et al., 2016. Thermal properties of sandstone after treatment at high temperature. Int. J. Rock Mech. Min. Sci. 85, 60–66. https://doi.org/10.1016/j.ijrmms.2016.03.006.
- Tze-Pin, L., Hood, M., Cooper, G.A., et al., 1992. Wear and failure mechanisms of polycrystalline diamond compact bits. Wear 156 (1), 133–150. https://doi.org/10.1016/0043-1648(92)90149-3.
- Wang, C., Li, S., Zhang, L., 2019. Evaluation of rock abrasiveness class based on the wear mechanisms of PDC cutters. J. Petrol. Sci. Eng. 174, 959–967. https:// doi.org/10.1016/j.petrol.2018.12.009.
- Warren, T.M., Sinor, L.A., 1994. PDC Bits: What's Needed to Meet Tomorrow's Challenge. SPE University of Tulsa Centennial Petroleum Engineering Symposium. SPE-27978-MS. https://doi.org/10.2118/27978-MS.
- Xu, X.C., Liu, Q.S., 2000. A preliminary study on basic mechanical properties for granite at high temperature. Chin. J. Geotech. Eng. 22 (3), 332–335.
- Xu, X.L., Gao, F., Zhang, Z.Z., et al., 2014. Energy and structural effects of granite after high temperature. Chin. J. Geotech. Eng. 36 (5), 961–968. https://doi.org/ 10.11779/CJGE201405022.
- Yahiaoui, M., Paris, J.Y., Delbé, K., et al., 2016a. Independent analyses of cutting and friction forces applied on a single polycrystalline diamond compact cutter. Int. J. Rock Mech. Min. Sci. 85, 20–26. https://doi.org/10.1016/j.ijrmms.2016.03.002.
- Yahiaoui, M., Paris, J.Y., Delbé, K., et al., 2016b. Quality and wear behavior of graded polycrystalline diamond compact cutters. Int. J. Refract. Metals Hard Mater. 56, 87–95. https://doi.org/10.1016/j.ijrmhm.2015.12.009.
- Yang, J., Fu, L.Y., Zhang, W., et al., 2019. Mechanical property and thermal damage factor of limestone at high temperature. Int. J. Rock Mech. Min. Sci. 117, 11–19. https://doi.org/10.1016/j.ijrmms.2019.03.012.
- Yang, S.Q., Ranjith, P.G., Jing, H.W., et al., 2017. An experimental investigation on thermal damage and failure mechanical behavior of granite after exposure to different high temperature treatments. Geothermics 65, 180–197. https:// doi.org/10.1016/j.geothermics.2016.09.008.
- Yang, X., Li, X., Lu, Y., 2011. Temperature analysis of drill bit in rock drilling. J. Cent. S. Univ. 10, 46–56.
- Zhang, B., Tian, H., Dou, B., et al., 2021. Macroscopic and microscopic experimental research on granite properties after high-temperature and water-cooling cycles. Geothermics 93, 102079. https://doi.org/10.1016/j.geothermics.2021.102079.
- Zhao, J., Wan, Z., Li, Y., et al., 2009. Research on granite cutting and breaking test under conditions of high temperature and high pressure. Chin. J. Rock Mech. Eng. 7, 1432–1438. https://doi.org/10.3321/j.issn:1000-6915.2009.07.017 (in Chinese).
- Zhao, Y., Feng, Z., Xi, B., et al., 2015. Deformation and instability failure of borehole at high temperature and high pressure in Hot Dry Rock exploitation. Renew. Energy 77, 159–165. https://doi.org/10.1016/j.renene.2014.11.086.
- Zhou, Y., Zhang, W., Gamwo, I., et al., 2017. Mechanical specific energy versus depth of cut in rock cutting and drilling. Int. J. Rock Mech. Min. Sci. 100, 287–297. https://doi.org/10.1016/j.ijrmms.2017.11.004.
- Zhu, X., Dan, Z., 2019. Numerical simulation of rock breaking by PDC bit in hot dry rocks. Nat. Gas. Ind. B 6 (6), 619–628. https://doi.org/10.1016/j.ngib.2019.04.007.
- Zijsling, D.H., 1987. Single cutter testing—A key for PDC bit development. SPE Offshore Europe Conference and Exhibition. SPE-16529-MS. https://doi.org/ 10.2118/16529-MS.